ISSN
2395-6992

International Journal of Engineering Research & Science

www.ijoer.com
www.adpublications.org

Volume-8! Issue-5! May, 2022 www.ijoer.com ! info@ijoer.com

Preface

We would like to present, with great pleasure, the inaugural volume-8, Issue-5, May 2022, of a scholarly journal, *International Journal of Engineering Research & Science*. This journal is part of the AD Publications series *in the field of Engineering, Mathematics, Physics, Chemistry and science Research Development*, and is devoted to the gamut of Engineering and Science issues, from theoretical aspects to application-dependent studies and the validation of emerging technologies.

This journal was envisioned and founded to represent the growing needs of Engineering and Science as an emerging and increasingly vital field, now widely recognized as an integral part of scientific and technical investigations. Its mission is to become a voice of the Engineering and Science community, addressing researchers and practitioners in below areas

Chemical Engineering	
Biomolecular Engineering	Materials Engineering
Molecular Engineering	Process Engineering
Corrosion Engineering	
Civil Engineering	
Environmental Engineering	Geotechnical Engineering
Structural Engineering	Mining Engineering
Transport Engineering	Water resources Engineering
Electrical Engineering	
Power System Engineering	Optical Engineering
Mechanical Engineering	
Acoustical Engineering	Manufacturing Engineering
Optomechanical Engineering	Thermal Engineering
Power plant Engineering	Energy Engineering
Sports Engineering	Vehicle Engineering
Software Engineering	
Computer-aided Engineering	Cryptographic Engineering
Teletraffic Engineering	Web Engineering
System Engineering	
Mathematics	
Arithmetic	Algebra
Number theory	Field theory and polynomials
Analysis	Combinatorics
Geometry and topology	Topology
Probability and Statistics	Computational Science
Physical Science	Operational Research
Physics	
Nuclear and particle physics	Atomic, molecular, and optical physics
Condensed matter physics	Astrophysics
Applied Physics	Modern physics
Philosophy	Core theories

Chemistry	
Analytical chemistry	Biochemistry
Inorganic chemistry	Materials chemistry
Neurochemistry	Nuclear chemistry
Organic chemistry	Physical chemistry
Other Engineering Areas	
Aerospace Engineering	Agricultural Engineering
Applied Engineering	Biomedical Engineering
Biological Engineering	Building services Engineering
Energy Engineering	Railway Engineering
Industrial Engineering	Mechatronics Engineering
Management Engineering	Military Engineering
Petroleum Engineering	Nuclear Engineering
Textile Engineering	Nano Engineering
Algorithm and Computational Complexity	Artificial Intelligence
Electronics & Communication Engineering	Image Processing
Information Retrieval	Low Power VLSI Design
Neural Networks	Plastic Engineering

Each article in this issue provides an example of a concrete industrial application or a case study of the presented methodology to amplify the impact of the contribution. We are very thankful to everybody within that community who supported the idea of creating a new Research with IJOER. We are certain that this issue will be followed by many others, reporting new developments in the Engineering and Science field. This issue would not have been possible without the great support of the Reviewer, Editorial Board members and also with our Advisory Board Members, and we would like to express our sincere thanks to all of them. We would also like to express our gratitude to the editorial staff of AD Publications, who supported us at every stage of the project. It is our hope that this fine collection of articles will be a valuable resource for *IJOER* readers and will stimulate further research into the vibrant area of Engineering and Science Research.

Mukesh Arora

(Chief Editor)

Board Members

Dr. M. Varatha Vijayan

Annauniversity Rank Holder, Commissioned Officer Indian Navy, Ncc Navy Officer (Ex-Serviceman Navy), Best Researcher Awardee, Best Publication Awardee, Tamilnadu Best Innovation & Social Service Awardee From Lions Club.

Dr. Mohamed Abdel Fatah Ashabrawy Moustafa

PhD. in Computer Science - Faculty of Science - Suez Canal University University, 2010, Egypt.

Assistant Professor Computer Science, Prince Sattam bin AbdulAziz University ALkharj, KSA.

Prof.S.Balamurugan

Dr S. Balamurugan is the Head of Research and Development, Quants IS & CS, India. He has authored/co-authored 35 books, 200+ publications in various international journals and conferences and 6 patents to his credit. He was awarded with Three Post-Doctoral Degrees - Doctor of Science (D.Sc.) degree and Two Doctor of Letters (D.Litt) degrees for his significant contribution to research and development in Engineering.

Dr. Mahdi Hosseini

Dr. Mahdi did his Pre-University (12^{th}) in Mathematical Science. Later he received his Bachelor of Engineering with Distinction in Civil Engineering and later he Received both M.Tech. and Ph.D. Degree in Structural Engineering with Grade "A" First Class with Distinction.

Dr. Anil Lamba

Practice Head – Cyber Security, EXL Services Inc., New Jersey USA.

Dr. Anil Lamba is a researcher, an innovator, and an influencer with proven success in spearheading Strategic Information Security Initiatives and Large-scale IT Infrastructure projects across industry verticals. He has helped bring about a profound shift in cybersecurity defense. Throughout his career, he has parlayed his extensive background in security and a deep knowledge to help organizations build and implement strategic cybersecurity solutions. His published researches and conference papers has led to many thought provoking examples for augmenting better security.

Dr. Ali İhsan KAYA

Currently working as Associate Professor in Mehmet Akif Ersoy University, Turkey.

Research Area: Civil Engineering - Building Material - Insulation Materials Applications, Chemistry - Physical Chemistry – Composites.

Dr. Parsa Heydarpour

Ph.D. in Structural Engineering from George Washington University (Jan 2018), GPA=4.00.

Dr. Heba Mahmoud Mohamed Afify

Ph.D degree of philosophy in Biomedical Engineering, Cairo University, Egypt worked as Assistant Professor at MTI University.

Dr. Aurora Angela Pisano

Ph.D. in Civil Engineering, Currently Serving as Associate Professor of Solid and Structural Mechanics (scientific discipline area nationally denoted as ICAR/08"–"Scienza delle Costruzioni"), University Mediterranea of Reggio Calabria, Italy.

Dr. Faizullah Mahar

Associate Professor in Department of Electrical Engineering, Balochistan University Engineering & Technology Khuzdar. He is PhD (Electronic Engineering) from IQRA University, Defense View, Karachi, Pakistan.

Prof. Viviane Barrozo da Silva

Graduated in Physics from the Federal University of Paraná (1997), graduated in Electrical Engineering from the Federal University of Rio Grande do Sul - UFRGS (2008), and master's degree in Physics from the Federal University of Rio Grande do Sul (2001).

Dr. S. Kannadhasan

Ph.D (Smart Antennas), M.E (Communication Systems), M.B.A (Human Resources).

Dr. Christo Ananth

Ph.D. Co-operative Networks, M.E. Applied Electronics, B.E Electronics & Communication Engineering Working as Associate Professor, Lecturer and Faculty Advisor/ Department of Electronics & Communication Engineering in Francis Xavier Engineering College, Tirunelveli.

Dr. S.R.Boselin Prabhu

Ph.D, Wireless Sensor Networks, M.E. Network Engineering, Excellent Professional Achievement Award Winner from Society of Professional Engineers Biography Included in Marquis Who's Who in the World (Academic Year 2015 and 2016). Currently Serving as Assistant Professor in the department of ECE in SVS College of Engineering, Coimbatore.

Dr. PAUL P MATHAI

Dr. Paul P Mathai received his Bachelor's degree in Computer Science and Engineering from University of Madras, India. Then he obtained his Master's degree in Computer and Information Technology from Manonmanium Sundaranar University, India. In 2018, he received his Doctor of Philosophy in Computer Science and Engineering from Noorul Islam Centre for Higher Education, Kanyakumari, India.

Dr. M. Ramesh Kumar

Ph.D (Computer Science and Engineering), M.E (Computer Science and Engineering).

Currently working as Associate Professor in VSB College of Engineering Technical Campus, Coimbatore.

Dr. Maheshwar Shrestha

Postdoctoral Research Fellow in DEPT. OF ELE ENGG & COMP SCI, SDSU, Brookings, SD Ph.D, M.Sc. in Electrical Engineering from SOUTH DAKOTA STATE UNIVERSITY, Brookings, SD.

Dr. D. Amaranatha Reddy

Ph.D. (Postdocteral Fellow, Pusan National University, South Korea), M.Sc., B.Sc. : Physics.

Dr. Dibya Prakash Rai

Post Doctoral Fellow (PDF), M.Sc., B.Sc., Working as Assistant Professor in Department of Physics in Pachhuncga University College, Mizoram, India.

Dr. Pankaj Kumar Pal

Ph.D R/S, ECE Deptt., IIT-Roorkee.

Dr. P. Thangam

PhD in Information & Communication Engineering, ME (CSE), BE (Computer Hardware & Software), currently serving as Associate Professor in the Department of Computer Science and Engineering of Coimbatore Institute of Engineering and Technology.

Dr. Pradeep K. Sharma

PhD., M.Phil, M.Sc, B.Sc, in Physics, MBA in System Management, Presently working as Provost and Associate Professor & Head of Department for Physics in University of Engineering & Management, Jaipur.

Dr. R. Devi Priya

Ph.D (CSE), Anna University Chennai in 2013, M.E, B.E (CSE) from Kongu Engineering College, currently working in the Department of Computer Science and Engineering in Kongu Engineering College, Tamil Nadu, India.

Dr. Sandeep

Post-doctoral fellow, Principal Investigator, Young Scientist Scheme Project (DST-SERB), Department of Physics, Mizoram University, Aizawl Mizoram, India- 796001.

Dr. Roberto Volpe

Faculty of Engineering and Architecture, Università degli Studi di Enna "Kore", Cittadella Universitaria, 94100 – Enna (IT).

Dr. S. Kannadhasan

Ph.D (Smart Antennas), M.E (Communication Systems), M.B.A (Human Resources).

Research Area: Engineering Physics, Electromagnetic Field Theory, Electronic Material and Processes, Wireless Communications.

Mr. Amit Kumar

Amit Kumar is associated as a Researcher with the Department of Computer Science, College of Information Science and Technology, Nanjing Forestry University, Nanjing, China since 2009. He is working as a State Representative (HP), Spoken Tutorial Project, IIT Bombay promoting and integrating ICT in Literacy through Free and Open Source Software under National Mission on Education through ICT (NMEICT) of MHRD, Govt. of India; in the state of Himachal Pradesh, India.

Mr. Tanvir Singh

Tanvir Singh is acting as Outreach Officer (Punjab and J&K) for MHRD Govt. of India Project: Spoken Tutorial - IIT Bombay fostering IT Literacy through Open Source Technology under National Mission on Education through ICT (NMEICT). He is also acting as Research Associate since 2010 with Nanjing Forestry University, Nanjing, Jiangsu, China in the field of Social and Environmental Sustainability.

Mr. Abilash

MTech in VLSI, BTech in Electronics & Telecommunication engineering through A.M.I.E.T.E from Central Electronics Engineering Research Institute (C.E.E.R.I) Pilani, Industrial Electronics from ATI-EPI Hyderabad, IEEE course in Mechatronics, CSHAM from Birla Institute Of Professional Studies.

Mr. Varun Shukla

M.Tech in ECE from RGPV (Awarded with silver Medal By President of India), Assistant Professor, Dept. of ECE, PSIT, Kanpur.

Mr. Shrikant Harle

Presently working as a Assistant Professor in Civil Engineering field of Prof. Ram Meghe College of Engineering and Management, Amravati. He was Senior Design Engineer (Larsen & Toubro Limited, India).

Zairi Ismael Rizman

Senior Lecturer, Faculty of Electrical Engineering, Universiti Teknologi MARA (UiTM) (Terengganu) Malaysia Master (Science) in Microelectronics (2005), Universiti Kebangsaan Malaysia (UKM), Malaysia. Bachelor (Hons.) and Diploma in Electrical Engineering (Communication) (2002), UiTM Shah Alam, Malaysia.

Mr. Ronak

Qualification: M.Tech. in Mechanical Engineering (CAD/CAM), B.E.

Presently working as a Assistant Professor in Mechanical Engineering in ITM Vocational University, Vadodara. Mr. Ronak also worked as Design Engineer at Finstern Engineering Private Limited, Makarpura, Vadodara.

Table of Contents

Volume-8, Issue-5, May 2022

Dimensional Evaluation of Miniaturized Parts Manufactured by 3D Printing

Gean Vitor Salmoria[1*], Manoella R. Cardenuto[2], Loise Silva[3]
Universidade Federal de Santa Catarina – Departamento de Engenharia Mecânica, Laboratório NIMMA
Caixa Postal 476, Florianópolis - SC - Brasil - CEP 88040-900
*Corresponding Author

Received: 04 May 2022/ Revised: 13 May 2022/ Accepted: 17 May 2022/ Published: 31-05-2022

Abstract**—** *The development of the manufacturing process to fabricate miniaturized components goes through aspects such as modifications of machines and tools, process optimizations, improvements in precision and accuracy, and fabrication of adapted geometries. Hot-embossing, laser abrasion, and microinjection molding are applicable methods of fabrication to a diversity of geometries and polymeric materials. Rapid prototyping and fabrication assist in the development of new products in a short amount of time with a reduction in costs, allowing the manufacturing of objects with tenths of millimeters and with an accuracy in the order of micrometers. 3D Printing process with photocurable resin is a recent method of rapid prototyping that is growing in the market. Intending to analyze how precise and accurate is the process of 3D printing of miniaturized models and analyze their dimensional tolerance, it was conducted a dimensional analysis of parts fabricated in a printer EDEN 250 by Objet. Qualitative results showed that EDEN 250 prints satisfactory small parts mainly with round formats. Parts with sharp edges show limitations regarding precision and accuracy. FullCure ® 720 is a resin with average quality since it absorbed moisture and is heat sensitive. Studied samples were classified according to the technical standard NBR 6158 as IT11 parts (max tolerance of ± 60 μm).*

Keywords— Rapid prototyping, 3D Printing, dimensional precision and accuracy.

I. INTRODUCTION

A change in part of the manufacturing industry of plastic components has been noticed, evidencing a tendency for miniaturization of devices and systems [1]. Market consolidation of miniaturized parts is demonstrated by the global growth between the years 2004 and 2009, from 12 billion to 25 billion dollars. It is known that the principal difficulty in the miniaturization of devices and parts is the existed limitation regarding precision and accuracy of fabrication processes. The development and adaptation of the manufacturing processes of miniaturized components go through aspects such as modifications in machines and tools, process optimization, improvements in precision and accuracy, and fabrication of adapted geometries [2][3]. The methods of miniaturization and micro-fabrication of polymeric components are an alternative with low cost for the technology of micro electromechanical system (MEMS) [4][5]. Hot-embossing, laser abrasion, and micro-molding by injection are applicable fabricated methods for a diversity of geometries and polymeric materials.

Prototyping and rapid-fabrication techniques as stereolithography (SL), selective laser sintering (SLS), and tridimensional printing (3DP) assist the development of new products in a short period with a reduction in costs [6][7]. These techniques allow the creation of objects in the range of hundreds to tenths of millimeters with an accuracy in the order of micrometers. EDEN 250 is a printer from Objet that allow the creation of models with layers of 0,016 mm and walls of 0,6 mm [8]. Intending to analyze how precise and accurate is the printing process of miniaturized models which are the dimensional tolerance according to ISO 286-2-1998, it was conducted an analysis of the dimensions of parts fabricated with the printer EDEN 250 from Objet based on the methodology developed for parts fabricated by SL in the Laboratory CIMJECT of the Department of Mechanical Engineering on the Federal University of Santa Catarina (UFSC) [9].

Rapid prototyping by 3D printing is a process similar of standard printers in which the printhead spurts ink in the paper. In the tridimensional printer a CAD model is created and loaded in the printer where the geometry is sliced, process similar with

any kind of equipment for rapid prototyping. A printhead with resin or binder, depending on the process, spurts the resin or the binder on the equipment tray building the prototype.

Currently, three companies manufacture equipment for rapid prototyping by 3D printing, Z Corporation, Objet, and 3D Systems.

The *Z Corporation* 3D Printer uses technology with binder powder. Firstly, the printer spreads a thin layer of powder, then the printhead prints a binder on the powder layer just deposited. Next, a piston presses the binder/powder layer leaving the surface flat and ready for the next material layer. Once the part is completed, the part is surrounded and supported by the powder that wasn't used on the part, powder that can be used for the next print.

Objet and *3D Systems* use a different process, both companies use UV photosensitive liquid resins which makes the prototypes more detailed. *Objet Geometrics* was the first company to work, with success, with photocurable polymers. In 2000, the development of the technology *Polyiet* allowed the rapid manufacturing of prototypes of different sizes, complex models, and high quality.

The working principle of this printer is as follows, a 3D model is developed in CAD software, and the project is converted to an STL or SLC (for the jewelry market) and then sliced. Eight printheads deposits simultaneously identical quantities of photocurable polymer on the printer tray on each movement along the x-axis, building a thin layer of polymer that is cured by the UV bulbs presented on the printer head.

When the first layer is completed, the tray moves along the z axis initiating a new layer. The process occurs successively until the model in finished. In this process, the model is ready to use when finished, without the need of post-cure. The process for support elimination is simple, the support resin can be dissolved by a brush or a jet of water and leaves no burrs [10]. Figure 1 shows a work scheme of the printer.

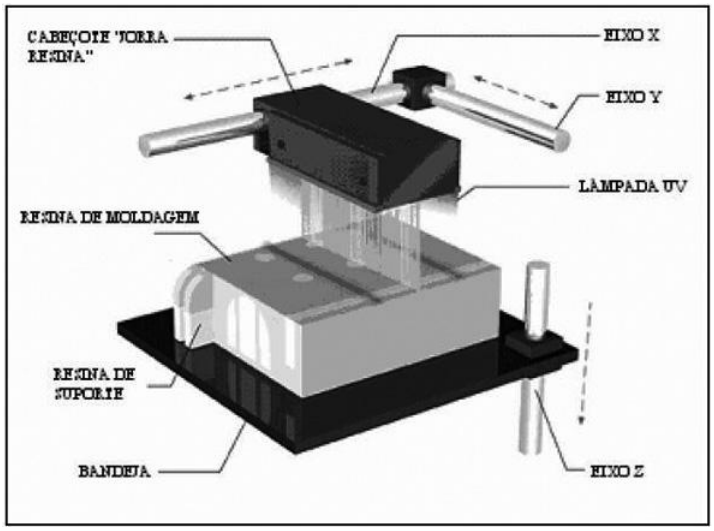

FIGURE 1: Work scheme of the printer 3D EDEN 250

Some of the advantages of the 3D EDEN 250 are high quality with layers with 0.016 mm of thickness resulting in models highly detailed and smooth. Resin properties allow walls and layers of 0.6 mm depending on the model. Allows an easy support elimination, no need of post-cure, variety of material properties and colors, and it allows the manufacture of more than one part each time, reducing production costs and time.

II. MATERIALS AND METHODS

2.1 Qualitative study

For the studies about the quality of miniaturized parts fabricated by 3D printing, a specimen with 112 x 60 x 3 mm, Figure 2, was project in a CAD software. The specimen was project with through holes with a variety of geometries (squares, circles, equilateral triangle and four-pointed star) and with dimensions between 500 µm and 10 mm. The parts were printed in a 3D EDEN 250 Printer with a FullCure® 720, epoxy and acrylic resin provide by the same manufacturer as the printer.

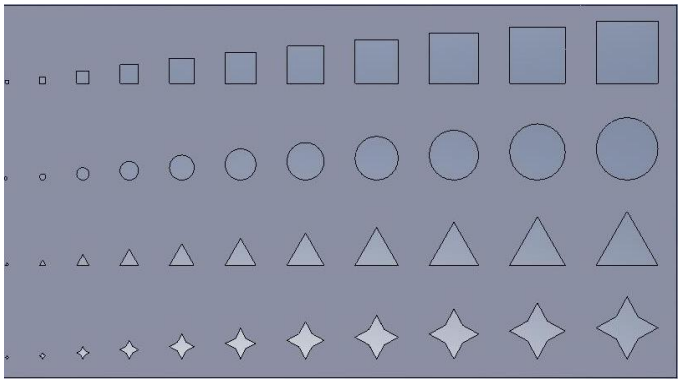

FIGURE 2: CAD Model of the part

Leica DMLM Microscopy was used to conduct the qualitative analysis of printed geometries.

2.2 Quantitative study

After the qualitative analysis, it was decided to proceed with a detailed study about the precision and/or accuracy of the prototypes printed in circular formats with 1.5 mm of diameter and quadrangular formats with lateral of 1.5 mm. Since it was not possible to have a complete visualization of the geometry with 1 mm on the minimum magnification of the equipment, it was printed geometries with 1.5 mm.

Geometries in triangular and star forms were discarded due to poor construction resulting in a considerable difficulty taking the measures.

Four specimens with 48 x 25,5 x 3 mm, 25 circulars through holes, and 25 quadrangular through holes were manufactured as well as four specimens with 74 x 36,5 x 4,5 mm, 25 circular pins, and 25 quadrangular pins. In total, 100 samples (between pins and holes) were printed and analyzed, as Figure 3. The pins have 3 mm in height and the holes have 3 mm in thickness.

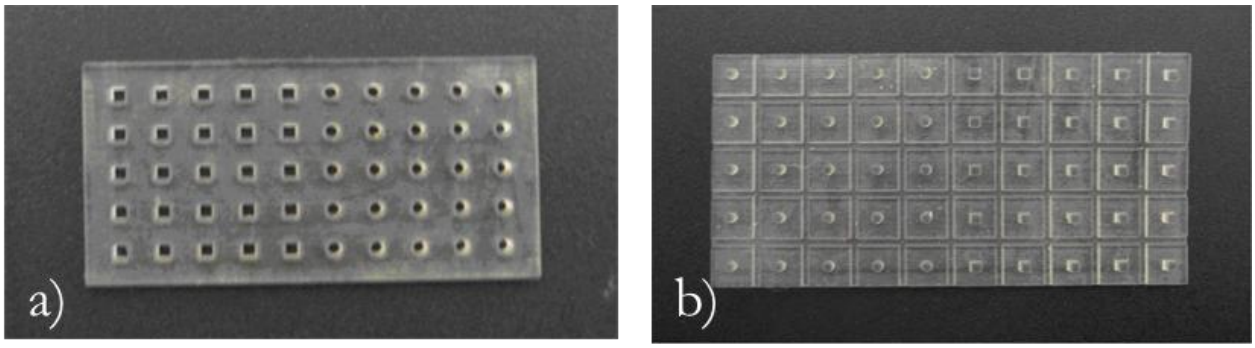

FIGURE 3: Specimens analyzed on the quantitative study. a) Part with holes b) Part with pins.

Pins measures were conducted with a microtome Mitutoyo Digimatic model MDC-25PJ. The through-holes were measured from images generated by a MO Leica – DMLM with a magnification of 5x and post-analysis in the software Adobe Photoshop CS3. Four diameter measures were taken in steps of 45° in all circular geometries, two measures in each lateral of the quadrangular geometries, and one in each diagonal.

III. RESULTS AND DISCUSSION

3.1 Qualitative study

In the manufacturing of holes with dimensions of 0.5 mm, the printer showed difficulty in building the geometries as projected by the CAD model. The printer wasn't able to print the holes with triangular and star formats of 0.5 mm size. Circular and square formats were printed, although the square format was not satisfactorily printed. The squares presented a format similar to circles.

Holes with circular, square, triangular, and star geometries with 1 mm dimensions were printed, but they showed a circular/oval geometry. Holes printed with 2 mm showed geometries as projected by CAD model. Figure 4 presents the images of the holes with 1 and 2 mm in the square and triangular formats.

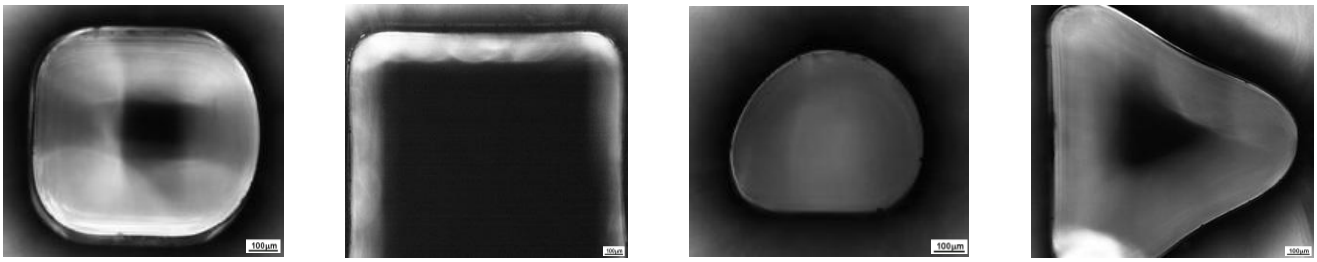

(a) (b) (c) (d)

FIGURE 4: Optic Microscopy of the printed holes. a) square with 1 mm. b) Square with 2 mm. c) Triangle with 1 mm. d) Triangle with 2 mm.

Figure 5 presents images of the holes with 10 mm. In the formats that have corners, the corners exhibit significative roundness even on the prints with 10 mm of dimension.

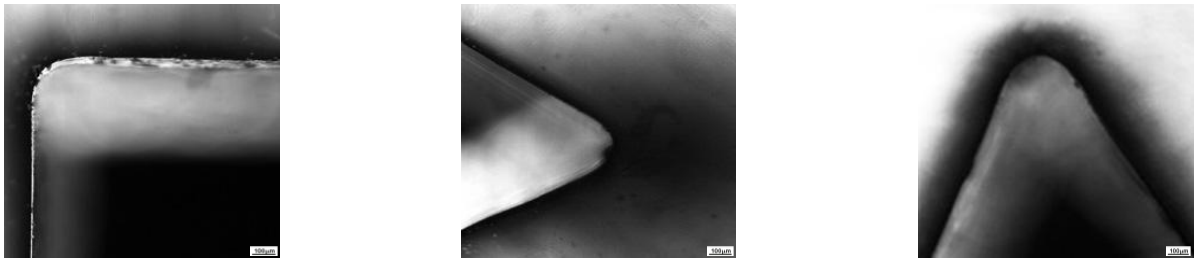

(a) (b) (c)

FIGURE 5: Optic Microscopy images of the corner of hole. a) Square with 10 mm. b) Triangle with 10 mm. c) Star with 10 mm.

3.2 Quantitative study

The two geometries printed presented a similar precision and accuracy behavior as shown in Tables 1 and 2. Since dimensions should have 1.5 mm, the square diagonal should have 2.121 mm.

When analyzing the holes, as shown in Table 1, the diameter average was 0.2 to 1.13 % below the diameter projected. The dimensions of the laterals were 1.5 to 1,8 % above the project, and the diagonals were 8.5 to 9.8 % below the expected.

TABLE 1
DIMENSIONS OF PRINTED HOLES

Holes		Circular	Squares	
		Diameter	Lateral	Diagonal
Specimen 1	Average (mm)	1,483	1,524	1,939
	Standard Deviation	0,012383	0,032195	0,024277
Specimen 2	Average (mm)	1,495	1,522	1,927
	Standard Deviation	0,016123	0,020444	0,017414
Specimen 3	Average (mm)	1,488	1,523	1,915
	Standard Deviation	0,028583	0,021456	0,018909
Specimen 4	Average (mm)	1,497	1,527	1,913
	Standard Deviation	0,013390	0,023041	0,016946

As shown in Table 2, the circular pins presented diameters 0.86 to 1.53% above the projected value. The laterals diverged from 3.46 to 4.13% above the expected and the diagonals between 6.6 % below to 5.23% above the CAD model.

The variation in the dimensions is because the printed samples in the square format presented round edges, as shown in section 3.1. For this reason, is noticed a more accentuated difference between the CAD model and the printed part.

TABLE 2
DIMENSIONS OF PRINTED PINS

Pinos		Circular	Square	
		Diâmetro	Lateral	Diagonal
Specimen 1	Average (mm)	1,513	1,562	2,001
	Standard Deviation	0,017202	0,030316	0,034433
Specimen 2	Average (mm)	1,518	1,552	2,010
	Standard Deviation	0,022647	0,036751	0,036498
Specimen 3	Average (mm)	1,519	1,554	1,981
	Standard Deviation	0,021990	0,036026	0,152309
Specimen 4	Average (mm)	1,523	1,562	2,010
	Standard Deviation	0,022723	0,035619	0,063927

IV. CONCLUSIONS

With qualitative results, it is possible to notice that EDEN 250 prints satisfactorily small parts, mainly with round formats. Parts with sharp corners do not perform as well as the round format, presenting poor precision and accuracy in the edges.

Even in bigger parts, with 100 mm, for example, the edges resolution is not satisfactory. The resin FullCure® 720 is a good resin for work, however it has high moisture absorption, and it is sensitive to heat.

Classifying the samples according with the technical standard NBR 6158, it is possible to classify the parts in the category IT11 (maximum tolerance of ± 0,06 mm). According with the experiments, the four specimens with circular and squares holes, had variation in the dimensions below the tolerance allowed, what demonstrate a great reliability in the printing process.

In the experiments with pins, most of the specimens presented variations below the maximum allowed. Specimens 1 and 4 of the square pins exceeded in 0.002 mm the tolerance allowed. Showing that the reliability of the printing process of square pins are 50%.

Analyzing the diagonals of the squares, all samples presented results above the maximum tolerance allowed, reaching 9.8% below the nominal size. Expected results due to the roundness of the sharp edges.

ACKNOWLEDGMENTS

The authors would like to thank FAPESC, CAPES, CNPq and FINEP for the financial support.

REFERENCES

[1] F. Batalha, G.; Cerveira, R.; Silva, Simulação de processos de microfabricação: influencia efeito de escala, n.d.

[2] W.K. Heckele, M.; Schomburg, Review on micro molding of thermoplastic polymers, J. Micromechanics Microengineering. (2003) R1–R14.

[3] J. Piotter, V.; Mueller, K.; Plewa, K.; Ruprecht, R.; Hausset, Performance and simulation of thermoplastic micro injection molding, Microsyst. Technol. (2004) 387–390.

[4] R.L.E. Brown, Design and manufacture of plastic parts, Wiley Intersci. (1980) 203.

[5] C.C. Zhou, J. G.; Herscovici, D.; Chen, Parametric process optimization to improve the accuracy of rapid prototyped stereolithography parts, Int. J. Mach. Tools Manuf. (1999) 363 – 379.

[6] P.F. Jacobs, Rapid Prototyping & Manufacturing: Fundamentals of Stereolitography, Soc. Manuf. Eng. (1992).

[7] P.F. Jacobs, Stereolithography and other RP&M Technologies, Soc. Manuf. Eng. (1996).

[8] Objet., (n.d.).

[9] P.Z. Salmoria, G. V.; Ahrens, Carlos Henrique; Lafratta, Fernando; Biava, Matheus Maragno; Ferreira, Rapid Manufacturing and Rapid Tooling of Polymer Micro Parts Using Stereolithography, J. Brazilian Soc. Mech. Sci. (2008).

[10] C.H. Salmoria, G.V.; Cardenuto, M. R.; Ahrens, Prototipagem rápida por impressão 3D com resinas fotocuráveis: uma análise sobre as tecnologias disponíveis no mercado nacional, in: CBPOL, 2007. An. Do 9o Congr. Bras. Polímeros., n.d.

Trimester-Specific Reference Intervals of Thyroid Function in Healthy Pregnant Women in Macau

Ka Wai CHOI[1*], Hoi Kei LEONG[2]

Department of Obstetrics and Gynecology, Kiang Wu Hospital, Macau Special Administrative Region, China
*Corresponding Author

Received: 08 May 2022/ Revised: 15 May 2022/ Accepted: 20 May 2022/ Published: 31-05-2022

Abstract—

Background: *To establish the trimester-specific reference intervals of thyrotropin (TSH), free thyroxine (FT4) and free triiodothyronine (FT3) in healthy pregnant women in Macau.*

Methods: *Serum samples were collected from 166 healthy pregnant Macau women since early pregnancy until the third trimester. The study was performed in Macau Kiang Wu Hospital from July 2020 to October 2021.Basic clinical and obstetrics data were gathered using questionnaires. Blood samples were sequentially collected from the pregnant women at the first (≤12weeks), the second (12-28 weeks) and the third (>28 weeks) trimesters, respectively.*

Result: *Reference intervals of TSH were 0.02~3.30mIU/L, 0.45~3.80mIU/L and 0.18~3.43mIU/L in three trimesters. For FT4, Reference intervals were 12.82~22.0pmol/L, 9.86~15.58pmol/L and 10.10~15.30pmol/L in three trimesters. For FT3, Reference intervals were 3.53~6.0pmol/L, 2.74~4.65pmol/L and 2.62~4.45pmol/L in three trimesters. The concentration of TSH was significant lower in the first trimester compared to the second and third trimesters of pregnancy (median o.89, 1.66, 1.41mIU/L); TSH concentration differences between trimesters are significantly different ($p<0.05$).FT4 values decreased with the progression of gestational period (median 16.60, 12.40, 12.15pmol/L). FT3 values decreased with the progression of gestational period (median 4.56, 3.65, 3.57pmol/L). FT4 and FT3 concentration had significantly differences between first and second trimesters ($p<0.05$), but had no significantly differences between second and third trimester ($p>0.05$).*

Conclusion: *This study is the first to establish trimester-specific reference intervals of TSH, FT4 and FT3 in healthy pregnant Macau women. Trimester-specific reference intervals may help in diagnosis and management of thyroid dysfunction during pregnancy which will prevent both maternal and fetal outcomes.*

Keywords— pregnancy, reference-intervals, thyroid hormone.

I. INTRODUCTION

Disease of the thyroid gland affects about 5% of the general population, and predominantly affects females [1]. During pregnancy, the thyroid gland increase in size by 10% in iodine-sufficient countries but by 20% to 40% in areas of iodine deficiency. Production of the thyroid hormones, thyroxine (T4), and triiodothyronine (T3), increases by nearly 50%, in conjunction with a separate 50% increase in daily iodine requirement. Normal thyroid function is essential for fetal development. The fetus is totally dependent on maternal thyroxine supply during the first trimester and second trimester for normal development and nerves system maturation. Because the progression of pregnancy and fetal, neonatal and child health are dependent on adequate thyroid hormones supplementation throughout pregnancy.A deficiency or an excess of thyroid hormone can occur in pregnancy. Thyroid dysfunction during pregnancy is common,with a prevalence of 2-4%. The prevalence of overt hyperthyroidism is approximately 0.1-0.4%, subclinical hyperthyroidism about 3.3% [2], overt hypothyroidism about 0.3%, and subclinical hypothyroidism may reach 2.5% or more, thyroid nodules about 3-21%[3]. Maternal thyroid dysfunction is association with an increased risk of various adverse maternal and child outcomes, including miscarriages , intrauterine growth retardation, anemia, abruption placenta, hypertensive disorders, preterm delivery,

postpartum hemorrhage, fetal distress, decreased child IQ and cognitive impairment in the offspring [4-6].Overt thyroid dysfunction is related with adverse obstetric outcomes and needs to be treated in pregnant women[7]. A large prospective cohort study suggested potential harmful effects of levothyroxine therapy on the child neurodevelopmental outcomes in pregnant women with subclinical hypothyroidism[8]. Because of a lack of specific clinical symptoms, subclinical hypothyroidism has to be defined by serum TSH concentration. Thus, the reference range of TSH is critical for diagnosis and treatment. Thyroid function reference ranges vary among different populations, with might be explained by variation in ethnicity, iodine intake, body mass index, and as well as assay methodology.It is important to determine reference intervals for normal thyroid function during pregnancy. Although several studies from different global regions,define reference ranges for thyroid hormones during pregnancy[9-14].Recent years, reference intervals of serum TSH reported for pregnant women in China have been reported[15-19], but China is a big country with large population, multi-ethnic and a variety of eating habits, peoples in south and the north are different in size, the reference intervals of serum TSH may be difference .For this reason, international guidelines for the diagnosis and management of thyroid disease during pregnancy recommend that trimester-specific reference intervals for TSH be calculated locally for each center in a population with optimal iodine intake.

II. MATERIALS AND METHODS

2.1 Study population

From July 2020 to October 2021, pregnant women who were attending Macau Kiang Wu Hospital for antenatal care since early pregnancy were enrolled. Analyses of thyroid function and thyroid antibodies were performed as part of their routine.

After explaining the purpose of the study, informed consent was obtained from each participants and the study was approved by the Research Ethics committee of the Macau Kiang Wu Hospital. On enrolment of participants, detailed history was enquired and participants were subjected to relevant general physical examination and findings were record on a predesigned form. Physical examination included the presence or absence of goiter and general and systemic examination.Salt has been iodized since 1994 and as a result, iodine intake in China is likely adequate Recruitment criteria included Chinese women residing in Macau for more than 10 years, age 19-40 years old, and single pregnancy at 7 to 12 weeks of gestation. Exclusion criteria applied to multiple pregnancies, patients with thyroid disease history or any other chronic diseases, diabetes, body mass index greater than 25 Kg/m^2, goiter on physical examination, positive of anti-thyroid peroxidase antibodies (TPOAb), TSH>10mIU/L, poor obstetrics history included 3 or more abortions, use of medications that can affect thyroid function, such as glucocorticoids, dopamine, or antiepileptic drugs, a history of thyroid surgery or radioactive iodine treatment.

Gestational age was determined by the last period and confirmed by ultrasound examination. When a major discrepancy between these two dates was found, the date of gestation was ultimately defined by ultrasound examination. Gestational age ≤12, 12-28 and >28 weeks comprised the first, second and third trimester of pregnancy. All the participants accepted sequential blood sampling once each trimesters.

2.2 Methods of sampling and laboratory testing

A morning fasting venous blood sample was obtained and isolated within 3 h of collection. Reference population was identified to calculate serum free triiodothyronine (FT3), free thyroxine (FT4), and TSH for each trimester of pregnancy, and autoantibodies (TPOAb) for first trimester of pregnancy only. The concentration of serum FT3, FT4, TSH and TPOAb were detected by an electrochemiluminescence immunoassay diagnostic kit (Roche Diagnostics Ltd, Basel, Switzerland) and analysed on Cobas E801 Module immunology analyser (Roche Diagnostics Ltd). Laboratory reference range for FT3, FT4, and TSH were 2.8-7.8pmol/L, 12-22pmol/L, and 0.27-4.2mIU/L, respectively. Normal range for TPOAb was <34 IU/ml and value greater than or equal to indicate elevated TPOAb in serum.

2.3 Statistical analysis

According to the aims and objectives of the study, the data were compiled and entered into MS Excel and analysed, using appropriate statistical test in SPSS software (version 22; SPSS Inc., Chicago, IL, USA). For descriptive statistics, frequencies, percentages, mean with standard deviations, and median of different variables were calculated. Data for TSH, FT3, and FT4 were expressed as median 2.5^{th}-97.5^{th} percentiles. One-Way analysis of variance (one-way ANOVA) was used to compare mean.

III. RESULTS

3.1 Baseline characteristics

From July 2020 to October 2021, 221 pregnant women were invited to participate in the study. We excluded 14 women who had positive thyroid autoantibodies, 7 women whose thyroid hormones were increased, 6 women who were abortion, 2 women whose foetuses had congenital deformities and needed abortion, 1 woman who refused to participate , 16 women who did not completed the study and 9 women who diagnosed of GDM in second trimester. Thus, a total of 166 participants were enrolled in the final study population. Flowchart of included/excluded pregnant women was showed in Fig. 1.

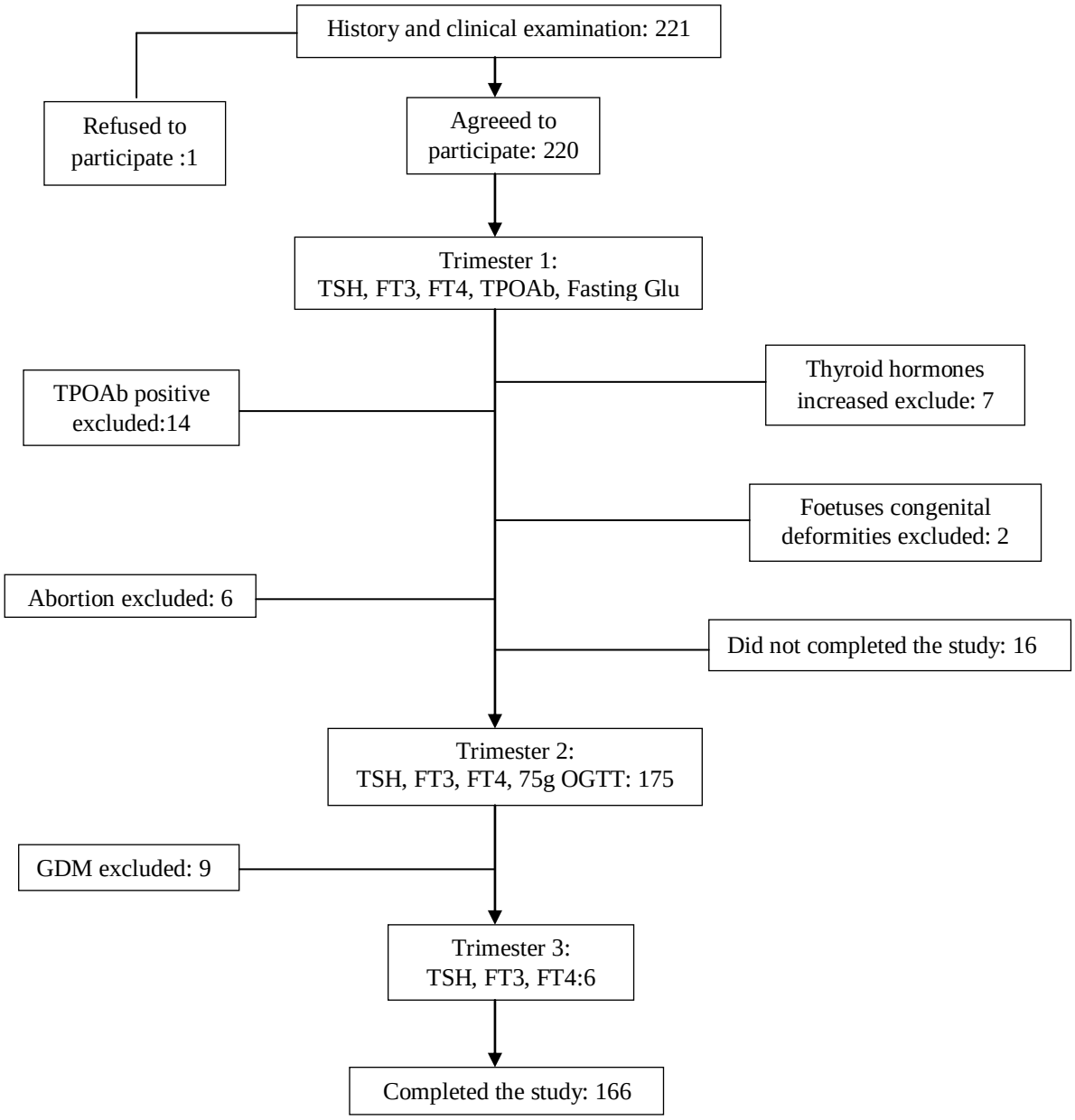

FIGURE 1: Flow chart of included/excluded pregnant women

The demographic, clinic, and obstetric characteristics of the 166 participants are described in Table 1. The mean age at study enrolment was 30.22(30±3.32) years, the range from 22~40 years old. Mean BMI was 20.14(19.95±2.37)Kg/m^2. Median TSH was 0.85, 1.66, 1.41mIU/L in each trimester. Median FT4 was 16.6, 12.4, 12.15pmol/L. Median FT3 was 4.57, 3.65, 3.57pmol/L.

TABLE 1
CLINICAL AND OBSTETRICAL CHARACTERISTICS OF THE STUDY POPULATION (n= 166)

Mean maternal age ± SD, years	30.22 ± 3.33
Maternal age	
20-25	11(6.63%)
26-30	84(50.60%)
31-35	60(36.14)
36-40	11(6.63%)
History of previous pregnancies, n (%)	
Nulliparous	82(49.40)
Parity 1	71(42.77%)
Parity ≥ 2	13(7.83%)
Smoker, n(%)	0
Mean BMI ± SD Kg/m2	20.14 ± 2.31
BMI range	15.7-28.9
Initial weight, n(%)	
Underweight(BMI< 18)	83(50%)
Normal weight (BMI: 18-24.9)	79(47.6%)
Overweight (BMI: 25-29)	4(2.4%)
Obesity (BMI ≥ 30)	0

Reference intervals of TSH, FT4, FT3 in each trimester

Reference intervals of TSH, FT4 and FT3 were defined as the range between 2.5th and 97.5th percentiles. Reference intervals of TSH were between 0.02 to 3.30mIU/L in the first trimester, 0.45 to 3.80mIU/L in second trimester, and 0.18 to 3.43 in third trimester. For FT4, Reference intervals were between12.82 to 22.0pmol/L in first trimester, 9.86 to 15.58pmol/L in second trimester, and 10.10 to 15.30pmol/L in third trimester. For FT3, Reference intervals were between 3.53 to 6.0mol/L in first trimester, 2.74 to 4.65pmol/L in second trimester, and 2.63 to 4.45pmol/L in third trimester. The reference interval (mean±standard deviation, median, 2.5th and 97.5th percentiles) for thyroidhormone levels in healthy pregnant Macau women was showed in Table 2.

TABLE 2
REFERENCE INTERVALS (mean±standard deviation, median, 2.5th and 97.5th percentiles) FOR THYROID HORMONE LEVELS IN HEALTHY PREGNANT MACAU WOMEN

Trimester	Hormones	Mean±SD	2.5th	5th	Median	95th	97.5th
First	TSH(mIU/L)	0.88±0.92	0.02	0.05	0.89	2.94	3.3
	FT4(pmol/L)	16.60±2.29	12.82	13.21	16.6	20.8	22
	FT3(pmol/L)	4.58±0.56	3.53	3.7	4.58	5.6	6
Second	TSH(mIU/L)	1.66±0.92	0.44	0.53	1.66	3.22	3.8
	FT4(pmol/L)	12.40±1.42	9.86	10.34	12.4	14.9	15.58
	FT3(pmol/L)	3.65±0.52	2.74	3	3.65	4.5	4.65
Third	TSH(mIU/L)	1.41±0.76	0.18	0.34	1.41	2.98	3.43
	FT4(pmol/L)	12.15±1.39	10.1	10.44	12.15	14.9	15.3
	FT3(pmol/L)	3.57±0.45	2.63	2.79	3.57	4.28	4.45

AS shown in Fig. 2, TSH values were suppressed in the first trimester, rose following the second trimester and supressed again in the third trimester. The concentration of TSH was significant lower in the first trimester compared to the second and third trimesters of pregnancy (median o.89, 1.66, 1.41mIU/L); TSH concentration differences between trimesters are significantly different ($p<0.05$). FT3 values decreased with the progression of gestational period (median 4.56, 3.65, 3.57pmol/L). FT3 concentration had significantly differences between first and second trimesters ($p<0.05$), but had no significantly differences between second and third trimester ($p>0.05$). FT4 values decreased with the progression of gestational period (median 16.60, 12.40, 12.15pmol/L). FT4 contraction decreased significantly from first trimester to second trimester ($p<0.05$), but the decreased from second trimester to third trimester was nonsignificant ($p>0.05$).

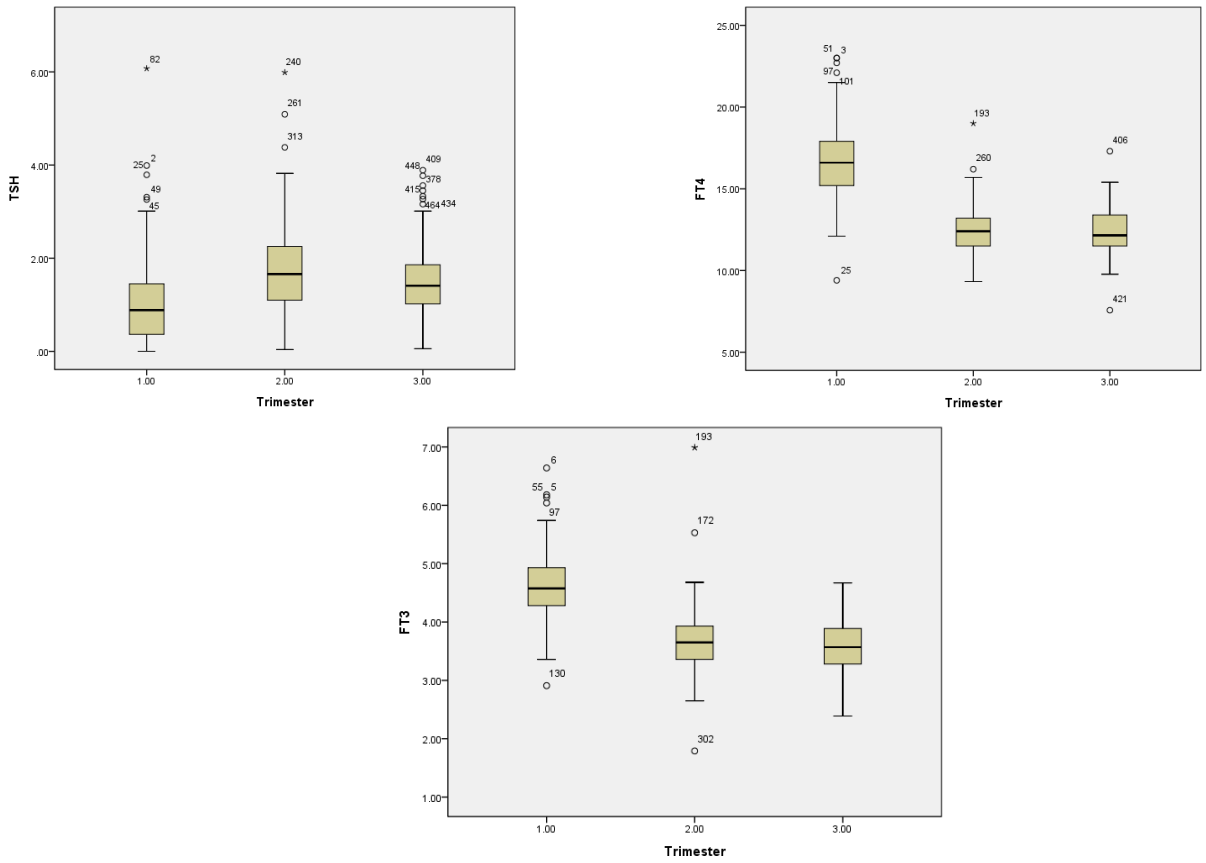

FIGURE 2: The concentrations of TSH, FT4, FT3. Data is presented as medians, interquartile range (box), non-outlier range (whiskers), and outliers (dots)

3.2 Prevalence of thyroid dysfunction

TPOAb was positive in 6.34% (14/220) of the participants. When the trimester-wise 2.5th to 97.5th percentile of TSH derived from the reference population in this study was applied to the total population with TPOAb(-), the number of women with subclinical hypothyroidism were 2(0,97%, 2/206) , hypothyroidism were 1(0.48%, 1/206), isolated hypothyroxinaemia were 3(1.36%, 3/206) in first trimester. The number of women with subclinical hypothyroidism were 5(2.86%, 5/175), isolated hypothyroxinaemia were 5(2.86%, 5/175) in second trimester. The number of women with subclinical hypothyroidism were 4(2.41%, 4/166), isolated hypothyroxinaemia were 2(1.20%, 2/166) in third trimester. There was no hypothyroidism case in second and third trimester.

IV. DISCUSSION

We recognized that pregnancy affects thyroid physiology, thereby leading to changes in thyroid parameters. As not only overt thyroid disease but also more subtle difference in thyroid hormone levels can lead to a wide range of complications in the mother and new-born. In pregnancy, a number of factors affect the determination of reference intervals for thyroid parameters. The most important definition is who healthy pregnant women are. Moreover, iodine saturation, different ethnics and analytical methods play a role. Clinical heterogeneity, test assay platform, thresholds used and quality features of the studies are likely to have contributed to the statistical heterogeneity observed.

2011 ATA guideline has recommended that when available, population- and trimester-specific reference ranges for serum TSH during pregnancy should be defined by a provider's institute of laboratory and should represent the typical population for whom care is provided. Reference ranges should be defined in healthy TPOAb-negative women with optimal iodine intake and without thyroid illness.

Macau is an iodine-sufficient city. In this study, we examined the thyroid parameters of same pregnant woman in ≤12, 12-28 and >28 weeks. Reference intervals of TSH in the present study were 0.02-3.30mIU/L during first trimester. As shown in Table 2, TSH reference in our study are comparable with some Western countries and India [9, 14, 25, 27], but lower compared with some other countries [10-13, 23, 24](Table 3).

TABLE 3
PREVIOUS REPORTS FROM OTHER COUNTRIES

Reference	Country	n	2.5th- 97.5th percentile
Bestwick et al(2014)	UK[9]	16334	0.06-3.50
Bestwick et al(2014)	Italy[9]	5505	0.04-3.19
Medici et al(2012)	Netherland[10]	5393	0.03-4.04
Marta et al(2017)	Poland[11]	172	0.009-3.177
Lorena et al(2016)	Chilean[12]	720	0.11-5.96
Kim et al(2016)	Korea[13]	417	0.03-4.24
Rajesh et al(2016)	India[14]	1430	0.37-3.69
Shrook et al(2019)	Egypt[23]	150	0.6-4.3
Fereidoun et al(2013)	Iran[24]	466	0.2-3.9
Joosen et al(2016)	Dutch[25]	60	~3.39
Almomin et al(2016)	Iraq[27]	893	0.04-3.77

If trimester-specific reference intervals for TSH are not available, 2011 ATA recommended the following reference intervals; 0.1-2.5mIU/L, 0.2-3.0mIU/L, 0.3-3.0mIU/L for first, second and third trimester. If using the upper limit reference of TSH, about 14(6.80%), 17(9.71%), 8(4.82%) pregnant women in the first, second and third trimester would be confirmed to be subclinical hypothyroidism. According to 2017 ATA guideline, the upper limit reference of TSH was 4mIU/L for first, second and third trimester. If using the new criteria, about 1 (6.80%) pregnant woman in the first trimester would be confirmed to be subclinical hypothyroidism. On the other hand, about 3(1.81%) pregnant women in the second trimester would be confirmed to be subclinical hypothyroidism. But, no pregnant woman was diagnosis of subclinical hypothyroidism in third trimester. The results of second-trimester reference range are closer to the values suggested by 2017 ATA for pregnant women than the TSH range in the first and third trimesters.

Since neither over diagnosis nor missed diagnosis is unacceptable, ATA propose that the local-specific reference is the best choice. If such reference is unavailable, than reference ranges from similar population using similar TSH assays will be the second choice. As shown in Table 4, in other Chinese Studies, the upper-limit reference of TSH in the first trimester is from 3.13 to 5.23mIU/L[15, 16, 18-22, 26, 28].TSH reference in our study within trimesters are comparable with Zhejiang, Shanghai and Sichuan [16, 19,22, 26], but significantly lower compared with some other provinces[15, 18, 20-21](Table 4).In this study, we tracking the TSH mean value for each trimester: we notice that the TSH value in the first trimester is lower than in the second trimester while the third trimester decreases again.

FT4 levels decrease as pregnancy progressed. This downward sloping curve in FT4 was also observed in many studies in China. In first trimester, the normal reference range of FT4 in our study is higher than studies of other coastal area of China. The reference intervals of FT4 in our study are consistent with Shenyang, Sichuan and Southwest [15, 26, 28], but higher than some other studies in China. Studies showed that hypothyroxinaemia in the early stages of pregnancy, is a predictor of lower IQ, language delay, worsened motor function, small head circumference, and an increased risk of autism [29-32]. In second trimester, the reference intervals of FT4 in our study are actually nearer to the values reported in Zhejiang and Sichuan, but different from some other studies in China

FT3 concentrations were significantly highest in the first trimester compared to the second and third trimester. Our data are consistent with the observations of Shen's study in Zhejiang [16].In our study, a maximum decrease in FT3 and FT4 was achieved in the second trimester, with no significant changes up to the end of pregnancy.

The populations of Zhang's study were living in Shenzhen where is very near Macau. But the reference ranges for thyroid hormones in normal pregnant women were significantly different [21].We therefore believe that even in women from the same geographical area, using the different methodological approach to calculating reference ranges, such reference ranges were highly laboratory-dependent and not applicable outside of its own clinical setting. In addition, it is known that, thyroid function is also affected by living habits, diet, and geographical location. In our population, people were in coastal area of China, while in Yang's , Shen's and Yang H's studies, the population were also from the coastal area of China and he reference range of thyroid hormone in healthy pregnant women had no significantly differences. The population of Ying's , Xing's and Chens studies were mainly from South-West of China, and in Li's study, the population was mainly from the North-East of China.

TABLE 4

TRIMESTER REFERENCE RANGE FROM DIFFERENT AREA OF CHINA

	Area	n	TSH(mIU/L)			FT4(pmol/L)			FT3(pmol/L)		
			Trimester1	Trimester 2	Trimester 3	Trimester 1	Trimester 2	Trimester 3	Trimester1	Trimester2	Trimester 3
Li	Shenyang[15]	640	0.10-4.34			12.3-20.88					
Shen	Zhejiang[16]	1409	0.16-3.78	0.34-3.51	0.34-4.32	10.9-17.7	9.3-15.2	7.9-14.1	2.9-5.0	2.9-4.6	2.9-4.5
Chen	Chengdu[18]	579	0.02-4.03	0.02-4.05	0.24-5.41	11.93-21.04	11.23-19.22	11.10-17.0	3.85-6.27	3.51-5.82	3.18-4.97
Yang H	Zhejiang[19]	3882	0.09-3.41	0.02-3.81		7.74-15.8	5.55-12.56				
Xing	Zhengzhou[20]	3314	0.07-3.96	0.07-3.96	0.27-4.53	9.16-18.12	8.67-16.21	7.80-13.90			
Zhang	Shenzhen[21]	2743	0.06-3.13	0.07-4.13	0.15-5.02	8.72-15.22	7.10-13.55	6.16-12.3			
Yang	Shanghai[22]	52027	0.03-3.52		0.39-3.67	11.7-19.7		9.1-14.4			
Wei	Sichuan[26]	150	0.08-3.29		0.81-4.33	11.88-20.06	9.89-15.8	9.22-15.77			
Ying	Southwest[28]	33040	0.02-5.23	0.03-5.24	0.37-5.68	11.66-20.69	10.1-18.59	9.85-16.86			
Our study	Macau	166	0.02-3.30	0.45-3.80	0.18-3.43	12.82-22.0	9.86-15.58	10.10-15.30	3.53-6.0	2.74-4.65	2.63-4.45

We performed a longitudinal study and the pregnant women were followed since early pregnancy until the third trimester. The trimester-specific ranges of TSH, FT4 and FT3 in our study are comparable with the studies from Dutch and China [19, 25,26]. But the sample size of our studies was limit and the same problems with the studies of Dutch and Wei et al. On the other hand, other studies use three different populations in three trimesters.

V. CONCLUSIONS

We found that the upper limit of serum TSH reference in the first trimester and second trimester were much higher than 2.5mIU/L and 3.0mIU/L in our population. On the other hand, the upper limit of serum TSH references in trimesters of our study was lower than 4mIU/L which proposed by ATA 2017 guideline. The trimester-specific reference ranges for serum TSH during pregnancy obtained from similar populations and maternal iodine status, but using different laboratory assay method were inconsistent. In conclusion, we established the trimester-specific reference intervals of TSH, FT4 and FT3 in TPOAb negative pregnant women from a tertiary care centre in Macau. In our opinion, measurement of TSH, FT4 and TPOAb in the systematic screening for thyroid dysfunctions in pregnancy is beneficial and it can help decide whether women should be treated with levothyroxine or not.

ACKNOWLEDGEMENTS

We would like to thank pregnant women in Macau, for their assistance with obtaining the data used in this study.

FUNDING

Funded by The Science and Technology Development Fund, Macau SAR government (File No. 0115/2019/A3)

DECLARATION OF INTEREST

The authors declare that there is no conflict of interest that could be perceived as prejudicing the impartiality of the research reported.

ETHICS APPROVAL AND CONSENT TO PARTICIPATE

Ethical clearance was approved by the Research Ethics committee of the Macau Kiang Wu Hospital. All enrolled participates signed a written consent form before they joined the study.

REFERENCES

[1] Strachan, M.W. J.; Newell-Price, J. Endocrine disease. In Davidson Principles and Practice of Medicine, 22nd ed. Walker, B. R., Ed.; Churchill Livingstone: Edinburg, UK, 2014; pp738-740.

[2] Rajput R, Goel V, Nanda S, et al. Prevalence of thyroid dysfunction among women during the first trimester of pregnancy at a tertiary care hospital in Haryana. Indian J EndocrinolMetab 2015; 19; 416-419.

[3] Alexander EK, Pearce EN, Brent GA, et al. 2017 Guidelines of the American Thyroid Association for the diagnosis and management of thyroid disease during and postpartum . Thyroid 2017; 27: 315-389

[4] Chan S, Boelaert K. Optimal management of hypothyroidism, hypothyroxinaemia and euthyroid TPO antibody positivity preconception and in pregnancy. ClinEndocrinol (Oxf) 2015; 82: 313-326.

[5] Negro R, Stagnaro-Green A . Diagnosis and management of subclinical hypothyroidism in pregnancy. BMJ 2014; 349: g4929.

[6] Medici M, Korevaar TI, Schalekamp-Timmermans S, et al. Maternal early-pregnancy thyroid function is associated with subsequent hypertensive disorders of pregnancy: the generation R study. The journal of clinical endocrinology and metabolism. 2014; 99(12): E2591-2598.

[7] Sheehan PM, Nankervis A, Araujo Junior E, et al. Maternal thyroid disease and preterm birth: systematic review and meta-analysis. J ClinEndocrinolMetab 2015; 100: 4325-4331.

[8] Korevaar TI, Muetzal R, Medici M, et al. Association of maternal thyroid function during early pregnancy with offspring IQ and brain morphology in childhood: a population-based prospective cohort study. Lancet Diabetes Endocrinol 2016; 4: 35-43.

[9] Bestwick JP, John R, Maina A, et al. Thyroid stimulating hormone and free thyroxine in pregnancy: expressing concentration as multiples of the median (MoMs). Clinicachimicaacta; international journal of clinical chemistry. 2014; 430: 33-37.

[10] Medici M, de Rijke YB, Peetes RP, et al. Maternal early pregnancy and newborn thyroid hormone parameters: the Generation R study. The Journal of clinical endocrinology and metabolism. 2012; 97(2): 646-652.

[11] Marta KM, Anna F, Ewa BA, et al. Reference values for TSH and free thyroid hormones in healthy pregnant women in Poland: A prospective, multicentre study. European Thyroid Journal. 2017; 6: 82-88.

[12] Lorena M, Alejandra M, Maria PR, et al. Early pregnancy thyroid hormone reference ranges in Chilean women: The influence of body mass index. ClinEndocrinol (Oxf). 2016 December; 85(6): 942-948.

[13] HJ Kim, YY Cho, SW Kim, et al. Reference intervals of thyroid hormones during pregnancy in Korea, an iodine-replete area. The Korean Journal of Internal medicine. 2018 May; 33(3)552-560.

[14] Rajesh R, Bhagat S, Vasudha G, et al. Trimester-specific reference interval for thyroid hormones during pregnancy at a tertiary care hospital in Haryna, India. Indian Journal of endocrinology and metabolism. 2016; 20(6): 810-815.

[15] Li C, Shan Z, Mao J, et al. Assessment of thyroid function during first- trimester pregnancy: What is the rational upper limit of serum TSH during the first trimester in Chinese pregnant women? J ClinMetab, 2014 January, 99(1): 73-79.

[16] Shen FX, Xie ZW, Lu SM , et al. Gestational thyroid reference intervals in antibody-negative Chinese Women. Clinical Biochemistry. 2014(47): 673-675.

[17] JX Fan, M Han, J Luo, et al. Reference intervals for common thyroid function tests, during different stage of pregnancy in Chinese Woman.Chin med J (Engl). 2013 Jul; 126(14): 2710-2714.

[18] YM Chen, J Zeng, YR Yan, et al. Reference intervals of thyroid hormones in normal pregnant women and effects of thyroid autoantibodies on thyroid hormones levels in pregnant women in Chengdu area. J Sichuan Univ (Med Sci Edi) 2017, 48(3): 450-454.

[19] Yang H, Shao ML, Chen LM, et al. Screening strategies for thyroid disorders in the first and second trimester of pregnancy in China. PLOS One. 2014 June, 9(6)e99611.

[20] Xing J, Yuan E, Li J et al. Trimester- and assay-specific thyroid reference intervals for pregnant women in China. Int J endocrinol 2016; 2016: 37554213.

[21] Zhang J, Li W, Chen QB et al. Establishment of trimester-specific thyroid stimulating hormone and free thyroxine reference interval in pregnant Chinese women using the Beckman Coulter UniCel^{TM}DxI 600. ClinChem Lab Med 2015; 53: 1409-1414.

[22] Yang Xi, Meng Yu, Zhang Yong, et al. Thyroid function reference ranges during pregnancy in a large Chinese population and comparison with current guidelines [J] . Chin Med J,2019,132 (5): 505-511.

[23] Shrook M, Shereen S, Maged A, et al.Trimester-specific thyroid hormone changes in normal pregnant Egyptian women. The Egyptian Journal of Internal Medicine , 2019, 31, 412-415.

[24] Fereidoun A, Ladan M, Atieh A, et al. Establishment of the trimester-specific reference range for free thyroxine index. Thyroid. 2013, 23(3): 354-359.

[25] Joosen AM, van der Linden IJ, de Jong-Aarts N, et al. TSH and ft4 during pregnancy: an observational study and a review of the literature. ClinChem Lab Med. 2016; 54(7): 1239-1246.

[26] Wei Q, Zhang L, Liu XX, et al. Clinical analysis of the specific referenceintervalsof the thyroid index for normal pregnant women. Zhonghua Fu Chan KeZaZhi, 2018, 25; 53(5): 299-303.

[27] Alomomin AMS, Mansour A, Sharief M. Trimester-specific reference intervals of thyroid function testing in pregnant women from Basrah, Iraq using electrochemiluminescent immunoassay. Disease 2016, 4(2):20.

[28] Ying G, Bin W, Wei D, et al. Establishment of trimester-specific reference interval for thyroid stimulating hormone and free thyroxine during pregnancy in Southwest China by direct method. Annals of clinical biochemistry: International Journal of laboratory medicine. 2021, DEC, 24.

[29] Lazarus JH, Bestwick JP, Channon S, et al. Antenatal thyroid screening and childhood cognitive function. N Eng J Med 2012,366: 493-501.

[30] Ong GS, Hadlow NC, Brown SJ, et al. Does the thyroid-stimulating hormone measured concurrently with first trimester biochemical screening tests predict adverse pregnancy outcomes occurring after 20 weeks gestation? J ClinEndocrinolMetab, 2014, 99: 2668-2672.

[31] Chen LM, Du WJ, Dai J, et al. Effects of subclinical hypothyroidism on maternal and perinatal outcomes during pregnancy: a single-center cohort study of a Chinese population. PloS One 9(10):e109364.

[32] Godoy GA, Korevaar TI, Peeters RP, et al. Materna; thyroid hormones during pregnancy, childhood adiposity and cardiovascular risk factors: the Genetation R study, ClinEndocrinol (Oxf), 2014, 81: 117-125.

Seismic Response Control of High Rise Mass Varied Structures using Friction Dampers

Arun Kumar G S[1*], Jagadish G Kori[2]

[*1]School of Civil Engineering, KLE Technological University, Huballi, India
Research Scholar at GEC Haveri, Visvesvaraya Technological University, Belagavi, India
[2]Civil Engineering Department, Government Engineering College, Haveri, India
Research Supervisor, Professor & Principal, Visvesvaraya Technological University, Belagavi, India
*Corresponding Author

Received: 10 May 2022/ Revised: 16 May 2022/ Accepted: 20 May 2022/ Published: 31-05-2022

Abstract— *When a seismic event causes unwanted motion in buildings, energy dissipation techniques in civil engineering are required. There are a variety of structures with passive energy dissipation provided by Passive Constant friction damper systems (CFRD). This technique is being used more and more to increase seismic protection for both existing and new constructions. The CFRD system results are explored in order to compare the structural response with and without this device of energy dissipation compared for low and high rise mass varied buildings, the damper put at different storey and altering the slip force has been focused in this study which gives an insight into the variation of slip load and its locations. The CFRD's potential to boost the structure's dissipative capacities without increasing stiffness was discovered. In the case of high-rise buildings, CFRD performance has been examined using top-storey displacements, allowing for a conclusion.*

Keywords— Constant Friction Damper, High Rise Buildings, Seismic Response, Slip load, Tall Structures.

I. INTRODUCTION

Tectonic plate movement's results in shaking of earth crust which will induce the waves like Primary, Secondary and Love waves on the earth's surface. Structures subjected to seismic excitation results in inertial forces [1] for mass of structure, inherent damping force of structure and resisting force by material stiffness, will try to curb the oscillation. As per IS 875 (Part-3):2015 based on height of structures classified as low and high rise, low rise structures due to stiffness can withstand and reduce the top storey displacement to some extent but not in the case of high rise or mass varying. Dampers which can be the solution for reducing the top storey displacements which it is classified into 4 categories like passive, semi-active, active and hybrid [2], in this study we focus on passive friction dampers [3]. Passive friction dampers are easy to install, effective in reducing energy from the system and requires frequent maintenance, in passive system of damping doesn't require any external power to dissipate seismic energy from the structure, also not required any sensors or external system to monitor, absorption of energy achieved by sliding one plate over another by means of clamping force , clamping force as increases will acts as a strut this phase is called as stick phase once the amount of force is greater than the clamping force from the structure then it will enters to slip phase where the resistance between two plates will be zero, the friction damper is purely displacement dependent device. A 3 [4] low rise and 11 [5] storey high rise benchmark mass varied buildings considered for the study using matlab as a tool by state space [6], frequency of the lumped mass models matches exactly with benchmark problems and hence study focused on reducing the top storey displacement for Elcentro 1940 earthquake for 5 g and 0.3417 g [7] accelerograms both the types of building, using passive friction damper at different location or storey's [8] in the building or structure, finding minimum numbers and location of dampers were discussed in this paper.

II. PASSIVE CONSTANT FRICTION DAMPERS

Passive friction dampers can be implemented in building was invented by Pall and Marsh in 1979 [9], initially it was used in the automobiles to decelerate by means of braking which a large part of kinetic energy dissipated in terms of heat. There are two major types of FRD (Friction Dampers) viz. Pall and Sumitomo friction dampers. FRD were experimentally efficient and it was proved by Skinner et. Al in 1975.

III. MECHANISM OF FRICTION DAMPER

Majorly the FRD works on clamping force, which decides the stick and slip phase of damper based on displacement allowed for the FRD. Parametric studies have shown that the slip load of the FRD plays a vital role, selecting the optimum slip load reduces maximum response of the structure, but ± 20% variation will not affect that much to response [10].

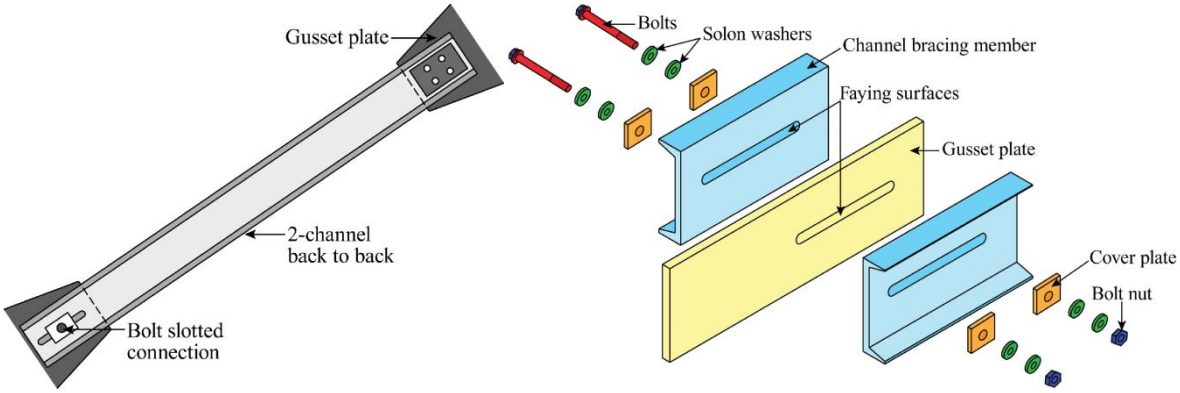

FIGURE 1: Anatomy of Passive Friction Damper [11]

Friction-based dampers consist of steel plates that are pulled together by high-strength bolts with axial or rotational deformation mechanisms to convert kinetic energy into thermal energy [12]. FRD functions similarly to fuses in that they limit the amount of force that can be applied to the structural members they protect. Because the hysteresis loop is rectangular, it dissipates the most of energy in a given force - displacement, regardless of velocity or frequency. Consistent and repeatable performance against a wide variety of earthquakes, with no maintenance required [13]. The value of damping force F is given by the relationship:

$$F_d = \pm\mu * N \tag{1}$$

Where,

F_d – Damping Force induced by Damper in Newton

μ - is the Coefficient of sliding friction between two plate surfaces, 0.60 for kinetic [14].

N - is Normal force across the moving surfaces also called as clamping force.

A typical force displacement relationship shown in below figure 2 of FRD, Structure and structure installed with FRD.

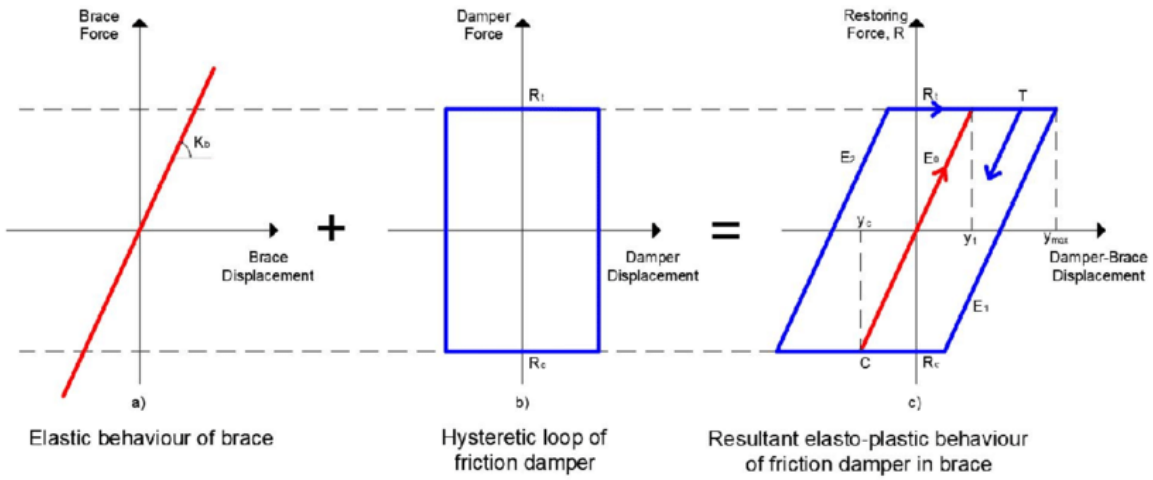

FIGURE 2: Hysteretic Curves of Brace, CFRD and CFRD Installed Structure [11]

The current study focuses on passive friction damping, the two important assumptions made for the study is that *nonlinearity* is concentrated only in FRD not in the structural members and FRD installed structure is to be treated as two different

systems to ensure elasto-plastic behaviour, the FRD will have two phases namely 'stick phase' and 'slip phase'[15]. In stick phase the damper acts as a braced frame (it is ignored in study) and once it reach the maximum value of friction force suddenly it will enters into slip phase where the behaviour of the damper changes from tension to compression or vice versa. The study uses only constant friction dampers (CFRD).

IV. GOVERNING EQUATIONS OF MOTION

Mathematically a structure can be modelled as a lumped mass at each storey with multi degree of freedom can be written as:

$$M * \ddot{x(t)} + C * \dot{x(t)} + K * x(t) = -M * \ddot{x(t)}_g \quad (2)$$

In the above equation if we add CFRD it can be rewritten as:

$$M * \ddot{x(t)} + C * \dot{x(t)} + K * x(t) + F_N = -M * \ddot{x}_g(t) \quad (3)$$

Where,

M – Mass matrix, diagonal matrix in kg

C – Damping matrix, tri-diagonal matrix in N-s/m

K – Stiffness matrix, tri-diagonal matrix in N/m

x(t) – Storey Acceleration vector due to excitation at that storey

x(t) – Storey Velocity vector due to excitation at that storey

x(t) – Storey Displacement vector due to excitation at that storey

xg(t) – Ground acceleration

V. NUMERICAL STUDY

The storey shear building frame model with and without friction damper at different storey's were modelled as linear lumped mass [16], governing equations of motion are stated above. The benchmark problem of 3 storey building configured with MR damper of passive off case [17] is considered with CFRD installed at ground storey. Using state space matrix it can be solved to determine the displacement and acceleration of the storey at the time t for the ground motion of NS component of El-centro 1940 data reproduced at 5 times the original record. The exact modelling of the problem using equations modelled in Matlab. System matrices are as mentioned below [18]:

$$Mass\ matrix = M = \begin{bmatrix} 98.3 & 0 & 0 \\ 0 & 98.3 & 0 \\ 0 & 0 & 98.3 \end{bmatrix} in\ kg$$

$$Damping\ matrix = C = \begin{bmatrix} 50 & -50 & 0 \\ -50 & 100 & -50 \\ 0 & -50 & 175 \end{bmatrix} in\ N-s/m$$

$$Stiffness\ matrix = K = (10^5) * \begin{bmatrix} 6.84 & -6.84 & 0 \\ -6.84 & 13.7 & -6.84 \\ 0 & -6.84 & 12 \end{bmatrix} in\ N/m$$

State Space matrices:

$$A = \begin{bmatrix} -M_i^{-1} * C_i & -M_i^{-1} * K_i \\ 0 & I \end{bmatrix} \qquad B = \begin{bmatrix} M_i^{-1} * \Gamma \\ 0 \end{bmatrix} \qquad E = -\begin{bmatrix} \Lambda \\ 0 \end{bmatrix}$$

State space output matrices:

$$C = \begin{bmatrix} 0 & 0 & 0 & 0 & 0 & 1 \\ -M_i^{-1} * C_i & & & -M_i^{-1} * K_i & & \end{bmatrix} \qquad D = \begin{bmatrix} 0 \\ M_i^{-1} * \Gamma \end{bmatrix}$$

Where,

$$Damper\ Location\ matrices = \Gamma = \begin{bmatrix} 0 \\ 0 \\ -1 \end{bmatrix} \qquad State\ matrices = \Lambda = \begin{bmatrix} 1 \\ 1 \\ 1 \end{bmatrix}$$

i =storey level

$$\dot{z} = A * z + B * F_d + E * \ddot{x_g} \qquad y = C * z + D * F_d$$

Validation or Comparison of results with the benchmark problem (BMP) considered as low rise structure [19]:

TABLE 1
COMPARISON OF STUDY RESULTS WITH BENCHMARK PROBLEM FOR LOW RISE CASE.

Parameter	Storey	Uncontrolled of BMP	Uncontrolled of study[18]	% of difference	Passive off case of BMP with MRD	CFRD installed model of study Target as top storey displ	% of difference
Storey Displacement in mm	Top - 1	9.62	9.647	0.28 %	4.55	4.579	0.63 %
	First - 2	8.20	8.246	0.56 %	3.57	3.500	1.96 %
	Ground - 3	5.38	5.407	0.50 %	2.11	2.011	4.69 %
	Base	0.0	0.0	0.0	0.0	0.0	0.0
Mean Difference				0.45 %			2.42 %
Slip Force in N (0.217 times of Storey weight)		-			258	210	19.20 %

Further the study continuous to keep the damper force constant of 258 N and observing the top storey displacement:

TABLE 2
COMPARISON OF STUDY RESULTS WITH BENCHMARK PROBLEM FOR LOW RISE CASE

Parameter	Storey	Passive off case of BMP with MRD	CFRD installed model of study	% of difference
Storey Displacement in mm	Top - 1	4.55	3.907	14.13 %
	First - 2	3.57	3.083	13.64 %
	Ground - 3	2.11	1.890	10.43 %
	Base	0.0	0.0	00.00 %
Mean Difference				12.73 %
Slip Force in N (As per Ref.)		258	258	0.00 %

Further the study continuous to locating CFRD at different storey's and the top storey displacement reduces from 9.647 to 4.55 mm for that clamping force or damper force 'f' results are listed as below:

TABLE 3
COMPARISON OF CFRD FORCE FOR CD VARIATION FOR DIFFERENT MODELS OF LOW RISE CASE.

Sl. No.	Model	Description	Damper Force in N	Top Storey Displ In mm
1	M-1	CFRD installed at ground storey only	210	4.579
2	M-2	CFRD installed at first storey only	210	3.323
3	M-3	CFRD installed at top storey only	210	2.344
4	M-4	CFRD installed at all storey	210	0.670
5	M-5	CFRD installed at ground & top storey only	210	1.349

The force displacement curves are as follows for the different models as mentioned in the above table:

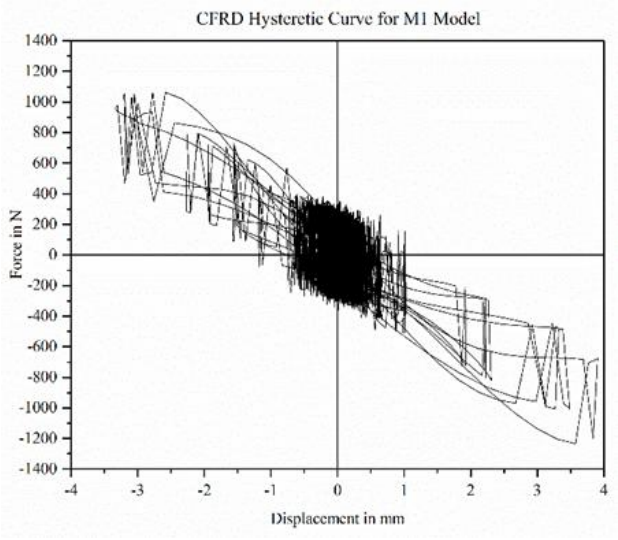

FIGURE 3: M1 model

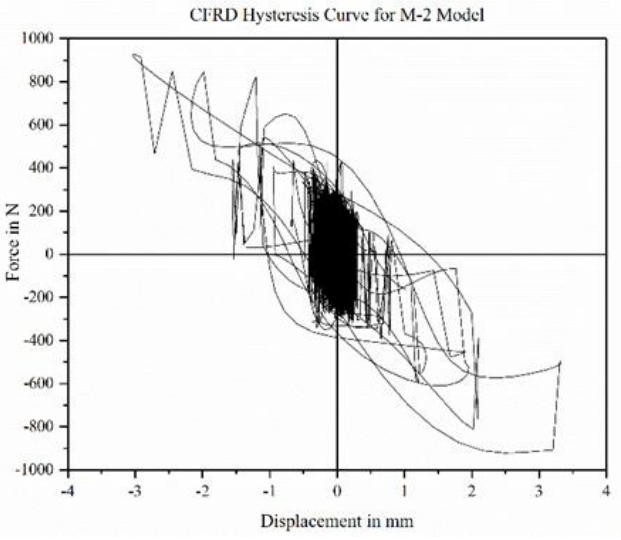

FIGURE 4: M2 model

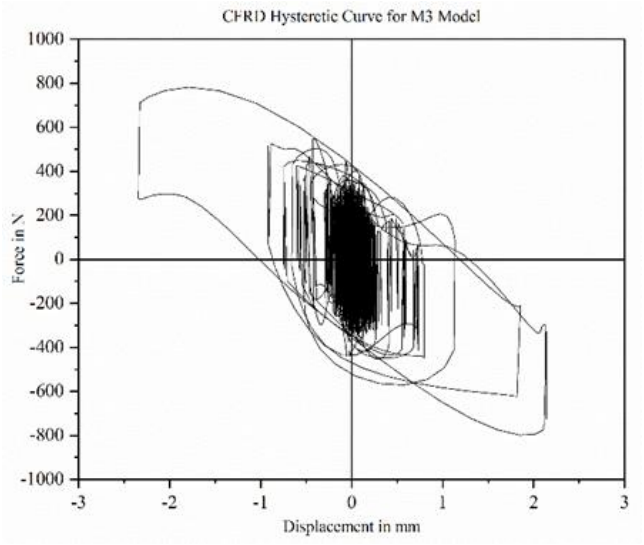

FIGURE 5: M3 model

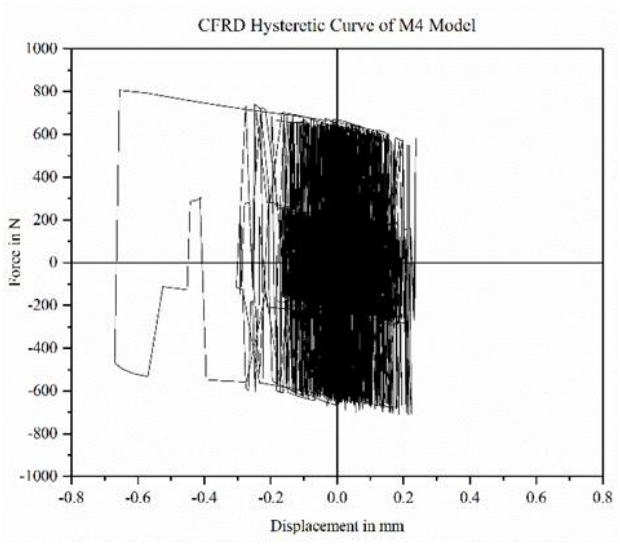

FIGURE 6: M4 model

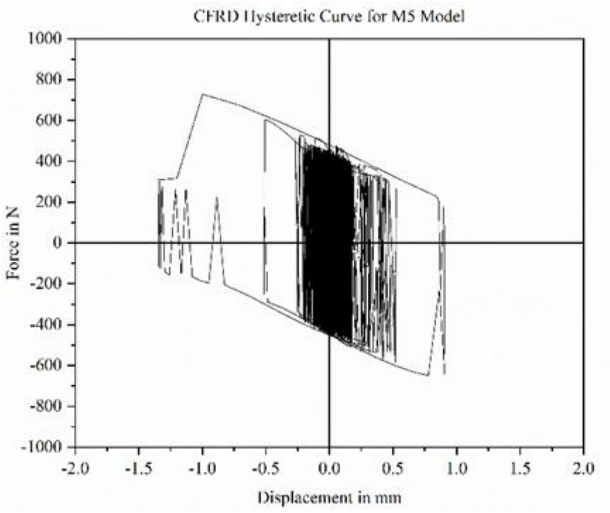

FIGURE 7: M5 model

Top storey displacement curve for NS component of Elcentro 1940 earthquake force for CFRD installed models:

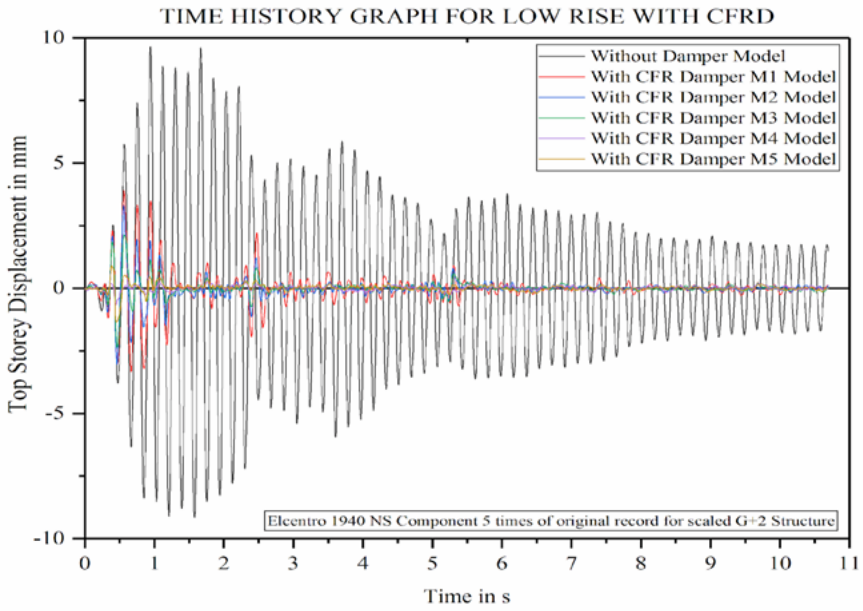

FIGURE 8: Top Storey displacement v/s time graph for constant friction damper.

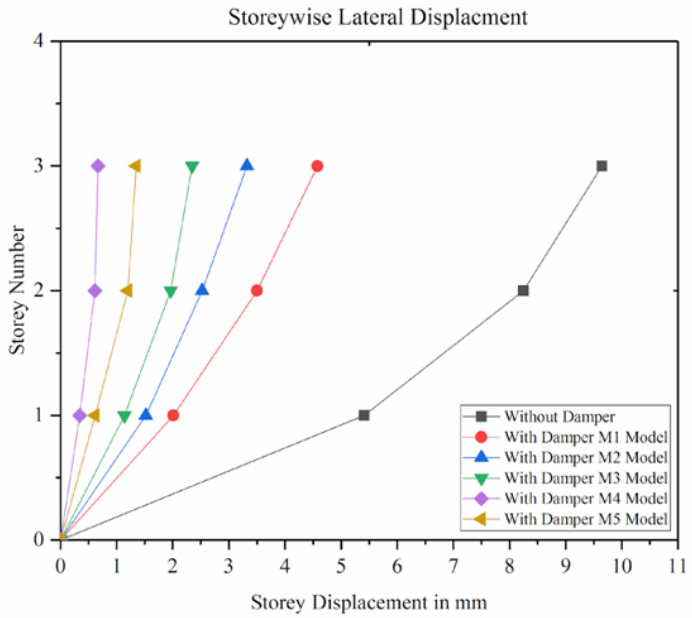

FIGURE 9: Lateral displacement for CFRD installed models

VI. HIGH RISE BUILDING

Further the study evaluates for the tall structure (high rise building 11 storey) [5], [19] are as follows:

$$Mass\ matrix = M = \begin{bmatrix} 1.76 & 0 & 0 & 0 & 0 & 0 & 0 & 0 & 0 & 0 & 0 \\ 0 & 2.03 & 0 & 0 & 0 & 0 & 0 & 0 & 0 & 0 & 0 \\ 0 & 0 & 2.03 & 0 & 0 & 0 & 0 & 0 & 0 & 0 & 0 \\ 0 & 0 & 0 & 2.03 & 0 & 0 & 0 & 0 & 0 & 0 & 0 \\ 0 & 0 & 0 & 0 & 2.01 & 0 & 0 & 0 & 0 & 0 & 0 \\ 0 & 0 & 0 & 0 & 0 & 2.01 & 0 & 0 & 0 & 0 & 0 \\ 0 & 0 & 0 & 0 & 0 & 0 & 2.01 & 0 & 0 & 0 & 0 \\ 0 & 0 & 0 & 0 & 0 & 0 & 0 & 2.00 & 0 & 0 & 0 \\ 0 & 0 & 0 & 0 & 0 & 0 & 0 & 0 & 2.01 & 0 & 0 \\ 0 & 0 & 0 & 0 & 0 & 0 & 0 & 0 & 0 & 2.01 & 0 \\ 0 & 0 & 0 & 0 & 0 & 0 & 0 & 0 & 0 & 0 & 2.15 \end{bmatrix} (1 * 10^5) in\ kg$$

$$Stiffness\ matrix = K$$

$$= (1 * 10^8)\begin{bmatrix} 3.12 & -3.12 & 0 & 0 & 0 & 0 & 0 & 0 & 0 & 0 & 0 \\ -3.12 & 7.49 & -4.37 & 0 & 0 & 0 & 0 & 0 & 0 & 0 & 0 \\ 0 & -4.37 & 8.74 & -4.37 & 0 & 0 & 0 & 0 & 0 & 0 & 0 \\ 0 & 0 & -4.37 & 8.74 & -4.37 & 0 & 0 & 0 & 0 & 0 & 0 \\ 0 & 0 & 0 & -4.37 & 8.87 & -4.50 & 0 & 0 & 0 & 0 & 0 \\ 0 & 0 & 0 & 0 & -4.50 & 9.00 & -4.50 & 0 & 0 & 0 & 0 \\ 0 & 0 & 0 & 0 & 0 & -4.50 & 9.00 & -4.50 & 0 & 0 & 0 \\ 0 & 0 & 0 & 0 & 0 & 0 & -4.50 & 9.00 & -4.50 & 0 & 0 \\ 0 & 0 & 0 & 0 & 0 & 0 & 0 & -4.50 & 9.18 & -4.68 & 0 \\ 0 & 0 & 0 & 0 & 0 & 0 & 0 & 0 & -4.68 & 9.44 & -4.76 \\ 0 & 0 & 0 & 0 & 0 & 0 & 0 & 0 & 0 & -4.76 & 9.44 \end{bmatrix} in\ N/m$$

$$Damping\ Matrix = C$$

$$= (1 * 10^6)\begin{bmatrix} 1.30 & -1.70 & 0 & 0 & 0 & 0 & 0 & 0 & 0 & 0 & 0 \\ -1.70 & 3.02 & -1.70 & 0 & 0 & 0 & 0 & 0 & 0 & 0 & 0 \\ 0 & -1.70 & 3.50 & -1.70 & 0 & 0 & 0 & 0 & 0 & 0 & 0 \\ 0 & 0 & -1.70 & 3.50 & -1.76 & 0 & 0 & 0 & 0 & 0 & 0 \\ 0 & 0 & 0 & -1.76 & 3.56 & -1.76 & 0 & 0 & 0 & 0 & 0 \\ 0 & 0 & 0 & 0 & -1.76 & 3.61 & -1.76 & 0 & 0 & 0 & 0 \\ 0 & 0 & 0 & 0 & 0 & -1.76 & 3.61 & -1.76 & 0 & 0 & 0 \\ 0 & 0 & 0 & 0 & 0 & 0 & -1.76 & 3.61 & -1.82 & 0 & 0 \\ 0 & 0 & 0 & 0 & 0 & 0 & 0 & -1.82 & 3.68 & -1.86 & 0 \\ 0 & 0 & 0 & 0 & 0 & 0 & 0 & 0 & -1.86 & 3.78 & -1.82 \\ 0 & 0 & 0 & 0 & 0 & 0 & 0 & 0 & 0 & -1.82 & 3.79 \end{bmatrix} in\ N - s/m$$

Validation or Comparison of results with the benchmark problem (BMP) considered as high rise structure:

TABLE 4
COMPARISON OF STOREY WISE DISPLACEMENT FOR HIGH RISE CASE [18].

Parameter	Storey	Uncontrolled of BMP [5]	Uncontrolled of study [18]	% of Difference
Storey Displacement in mm	11	147.0	148.26	0.86
	10	140.0	144.62	3.30
	9	140.0	139.10	0.64
	8	130.0	130.80	0.62
	7	120.0	119.88	0.10
	6	100.0	106.95	6.95
	5	90.0	91.97	2.18
	4	74.0	75.23	1.66
	3	57.0	57.06	0.10
	2	39.0	38.53	1.20
	1	19.0	19.62	3.26
	0	0.00	0.00	0.00
Mean Difference				1.90 %

Constant Friction Damper parameters: Clamping force N = 25 kN, Slip force = 0.6*N = 15 kN [20]

Model 1: Dampers Installed at all storey's

TABLE 5
COMPARISON OF STOREY WISE DISPLACEMENT FOR CFRD INSTALLED AT ALL STOREY FOR HIGH RISE CASE.

Storey No.	Storey Displacement for without Damper in mm [5]	Storey Displacement for with Damper in mm	% reduction	CFRD force Developed in Damper in kN
11	148.2	49.17	66.82%	15 in each storey
10	144.6	47.03	67.48%	
9	139.1	44.26	68.18%	
8	130.8	40.60	68.96%	
7	119.8	36.60	69.45%	
6	106.9	32.71	69.40%	
5	91.9	28.86	68.60%	
4	75.2	24.78	67.05%	
3	57.0	19.85	65.18%	
2	38.5	13.97	63.71%	
1	19.6	7.27	62.91%	
0	0.00	0.00	0.00	-

Model 2: Dampers Installed at alternate storey's

TABLE 6
COMPARISON OF STOREY WISE DISPLACEMENT FOR CFRD INSTALLED AT ALTERNATE STOREY FOR HIGH RISE CASE.

Storey No.	Storey Displacement for without Damper in mm [5]	Storey Displacement for with Damper in mm	% reduction	Force Developed in Damper in kN
11	148.2	57.23	61.38%	15
10	144.6	54.67	62.19%	-
9	139.1	51.36	63.08%	15
8	130.8	47.39	63.77%	-
7	119.8	43.96	63.31%	15
6	106.9	41.09	61.56%	-
5	91.9	37.15	59.58%	15
4	75.2	31.95	57.51%	-
3	57.0	25.33	55.56%	15
2	38.5	17.69	54.05%	-
1	19.6	9.17	53.21%	15
0	0.00	0.00	0.00	-

Model 3: Dampers Installed at alternate two storey's

TABLE 7
COMPARISON OF STOREY WISE DISPLACEMENT FOR CFRD INSTALLED AT ALTERNATE TWO STOREY FOR HIGH RISE CASE.

Storey No.	Storey Displacement for without Damper in mm [5]	Storey Displacement for with Damper in mm	% reduction	Force Developed in Damper in kN
11	148.2	88.93	39.99%	-
10	144.6	86.70	40.04%	15
9	139.1	83.38	40.06%	-
8	130.8	78.37	40.08%	-
7	119.8	71.76	40.10%	15
6	106.9	63.98	40.15%	-
5	91.9	54.97	40.18%	-
4	75.2	44.91	40.28%	15
3	57.0	34.03	40.30%	-
2	38.5	22.96	40.36%	-
1	19.6	11.67	40.46%	15
0	0.00	0.00	0.00	-

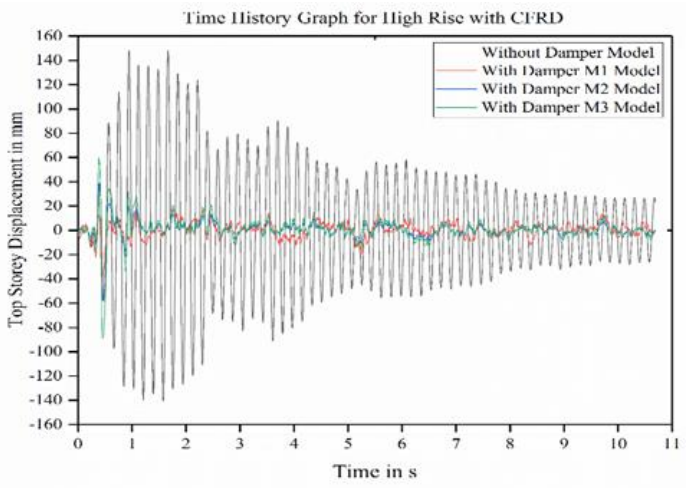

FIGURE 10: Top Storey displacement v/s time graph for with and without dampers

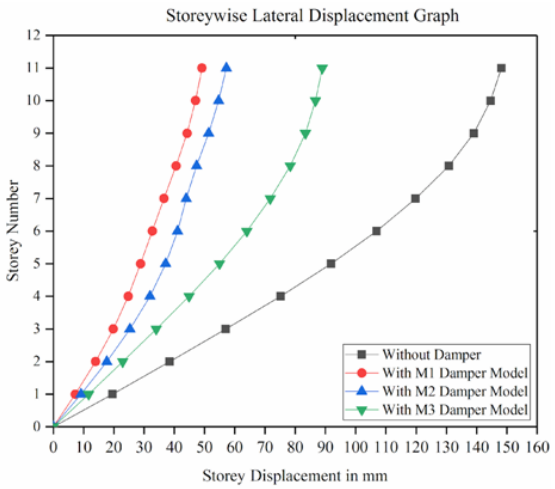

FIGURE 11: Lateral displacement for CFRD installed models

VII. RESULTS & DISCUSSIONS

Low Rise Case:

1. Validating benchmark problem to 0.45 % difference in results led to the conclusion that modelling of the structure is effective.
2. When the friction force is constant hysteretic curves are almost rectangular.
3. When the CFRD numbers varied in buildings force developed by damper is constant.
4. The M-4 model acquired the lowest top storey displacement, but it is uneconomical, thus the M-5 model fetched the next better results when compared to the M-4 and M-5 models, as shown in table 3.

5. Models without dampers follow a linear pattern as seen in fig.2, whereas M-2 to M-5 models follow a hysteretic curve.
6. Slip load of 0.217 times of storey weight considered and obtained less force generated by the damper when compared with BMP.

High Rise Case:

1. The 11-story high rise mass and stiffness have been varied as it rises.
2. The friction force kept constant here based on the storey shears.
3. The lateral displacement curve is parabolic as per the fig.16.
4. The tall structure's average storey-wise displacement difference is 1.90%..
5. When CFRD are put at different places in tall structures, as mentioned in tables 5, 6, and 7, the number of dampers as high as the storey displacements are likewise minimal.
6. When compared to WOD, the optimum models for tall structures are dampers put at alternative 2 storeys with fewer dampers but up to 40% lower displacements achieved.

VIII. CONCLUSIONS

1. Mass kept same in all storey's with CFRD to reduce the top storey displacements required 19 % less force compared to BMP.
2. Mass and stiffness are varied with CFRD to reduce top storey displacements upto 40 %.
3. It is nearly hard to maintain the same mass throughout all storeys in real time.
4. CFRD at two alternate storey in low and high rise cases shows good results when compared to CFRD installed at all storey's.

REFERENCES

[1] G. B. M., "Principia Mathematica," *Nature*, vol. 87, no. 2183. pp. 273–274, 1911, doi: 10.1038/087273a0.

[2] T. E. Saaed, G. Nikolakopoulos, J. E. Jonasson, and H. Hedlund, "A state-of-the-art review of structural control systems," *JVC/Journal of Vibration and Control*, vol. 21, no. 5, pp. 919–937, 2015, doi: 10.1177/1077546313478294.

[3] D. P. Taylor, "History, design, and applications of fluid dampers in structural engineering," *Passive Structural Control Symposium, 13-14 December, Tokyo Institute of Technology, Japan*, pp. 17–34, 2002, [Online]. Available: http://taylordevices.com/papers/history/design.htm.

[4] S. J. Dyke and B. F. Spencer, "A comparison of semi-active control strategies for the MR damper," *Proceedings - Intelligent Information Systems, IIS 1997*, no. January 1998, pp. 580–584, 1997, doi: 10.1109/IIS.1997.645424.

[5] S. Pourzeynali, H. H. Lavasani, and A. H. Modarayi, "Active control of high rise building structures using fuzzy logic and genetic algorithms," *Engineering Structures*, vol. 29, no. 3, pp. 346–357, 2007, doi: 10.1016/j.engstruct.2006.04.015.

[6] R. L. W. Ii *et al.*, *Linear State-Space Control Systems*. 2007.

[7] B. Halldórsson, G. P. Mavroeidis, and A. S. Papageorgiou, "Near-fault and far-field strong ground-motion simulation for earthquake engineering applications using the specific barrier model," *Journal of Structural Engineering*, vol. 137, no. 3, pp. 433–444, 2011, doi: 10.1061/(ASCE)ST.1943-541X.0000097.

[8] M. P. Singh and L. M. Moreschi, "Optimal placement of dampers for passive response control," *Earthquake Engineering and Structural Dynamics*, vol. 31, no. 4, pp. 955–976, 2002, doi: 10.1002/eqe.132.

[9] R. S. P. PALL, AVATAR S PALL, "*Friction Dampers for Seismic Control of Buildings 'A Canadian Experience,'" In 11th World Conference on Earthquake Engineering*, 1996, pp. 497–505.

[10] A. Pall and R. T. Pall, "13 th World Conference on Earthquake Engineering *Performance-Based Design using Pall Friction Dampers - An Economical Design Solution.*," no. 1955, 2004.

[11] V. M. Suhasini Madhekar, Passive Vibration Control of Structures. Newyork: Taylor & Francis, 2022.

[12] T. H. Babak ESMAILZADEH HAKIMI, Alireza RAHNAVARD, "SEISMIC DESIGN OF STRUCTURES USING FRICTION DAMPER BRACINGS," in *13th World Conference on Earthquake Engineering*, 2004, pp. 1–6.

[13] C. Marsh, "The control of building motion by friction dampers," *12th World Conference on Earthquake Engineering*, pp. 1–6, 2000.

[14] J. F. Sullivan, "THE PHYSICS FACT BOOK." https://hypertextbook.com/facts/2005/steel.shtml.

[15] H. M. Aktan, "Abating earthquake effects on buildings by active slip brace devices," *Shock and Vibration*, vol. 2, no. 2, pp. 133–142, 1995, doi: 10.3233/SAV-1995-2204.

[16] M. Paz and W. Leigh, "Structural Dynamics Theory and Computation By Mario Paz." 2004.

[17] S. J. Dyke, B. F. Spencer, M. K. Sain, and J. D. Carlson, "Modeling and control of magnetorheological dampers for seismic response reduction," *Smart Materials and Structures*, vol. 5, no. 5, pp. 565–575, 1996, doi: 10.1088/0964-1726/5/5/006.

[18] A. K. G. S and J. G. Kori, "Seismic Response Control of High-Rise Mass Varied Structures Using Linear Fluid Viscous Damper," no. May, 2022.

[19] IS: 875 (2015), "Indian Standard design loads (other than earthquake) for buildings and structures-code of practice,part 3(wind loads)," *BIS, New Delhi*. p. 51, 2015.

[20] M. Armali, J. Hallal, and M. Fakih, "Effectiveness of friction dampers on the seismic behavior of high rise building VS shear wall system," no. November, pp. 1–14, 2019, doi: 10.1002/eng2.12075.

Instrumental Characterization of Bull's (Red Bororo) Bloodmeal from its Fresh Sample

Izunna Ijezie Asoegwu[1], Ejikeme Emenike Emmanuel[2], Maduegbuna John Ikedinachukwu[3], C.O Umobi[4]

Department of Agricultural and Bioresources Engineering, Nnamdi Azikiwe University, Awka, Anambra State, Nigeria

Received: 25 April 2022/ Revised: 10 May 2022/ Accepted: 17 May 2022/ Published: 31-05-2022

Abstract— *The chloro compound, Ethene, Amine, Carbonyl compound, cyanide and methylene compounds were assigned 889.9796 cm^{-1}, 1401.735 cm^{-1}, 1627.371 cm^{-1}, 2208.360 cm^{-1}, 2445.666 cm^{-1} and 2600.767 cm^{-1} respectively. Methylene has a weak band, making it less prominent in Bull's bloodmeal. The fresh blood and dried blood of a red Bororo male cattle was subjected to infra-red spectroscopy at Spring board laboratory, Awka, Anambra State, Nigeria. The interactive effects due to the functional groups during drying were responsible for the changes observed in the spectra. It can be deduced that the dried sample has a more stable and sharper bands than those of the fresh sample. The infra-red spectrum of the bloodmeal consists of several peaks. At the region of N-H stretches, the peak looks like a cow udder, confirming the presence of primary amine.*

Keywords— Blood, Bloodmeal, Amine, Amino acid, Protein, Functional group, Peak.

I. INTRODUCTION

Bloodmeal is a dry inert powder used as a high protein livestock feed. Bloodmeal contains fat, fibre, ash etc. It also contains lysine, calcium, isoleucine, phosphorus and Methionine. It is imperative to note that the notable feature of raw blood is its high content of moisture. Food materials with high moisture content are liable to deteriorate easily. Raw blood must be processed before being incorporated into animal feeds. Blood from animals has recorded widespread applications especially in the food industry. Blood has been used as emulsifiers, to make blood sausages, blood curd, bread and blood pudding, blood cake and biscuits (Hsieh and Ofori, 2011 and Damba, 2017). As a result of limitation on blood applicability in the food industry from consumers, cultural and religious perceptions, blood has found applications in other industrial applications (Damba, 2017). These applications include animal feed as supplement and dietary enricher, food industry as emulsifier and thickener, fertilizers as pH stabilizer and seed coating, laboratory as culture media and protein source, medical, pharmaceutics as cosmetics and industry as adhesive, insecticide coadjutant, plastic additive, etc. (Davila Ribot, 2007).

Due to the scarcity of protein feedstocks in animal feeds formulation, Bloodmeal adoption, in the formulation of livestock feeds, as a protein source becomes highly imperative. This is majorly because of the availability of blood from abattoirs that can easily be dried. Donkoh *et al*, (1999) posits that the re-appraisal of optimum inclusion rate, and a recognition that balanced amino acid can improve livestock performance. Amine-group-containing species are amino acids and their polymers. The chemistry of amino acid side chains is critical to protein structure. Proteins are large biological molecules made up of long chains of smaller molecules called amino acids. Amino acids are organic molecules that contain an amine functional group (-NH_2), a carboxylic acid (-COOH). The presence of amines in bloodmeal makes bloodmeal a high protein animal feedstock.

II. FRESH BULL BLOOD SAMPLE CHARACTERIZATION

The plot of the Fourier transform infra-red spectroscopy of the fresh sample of the cow blood is presented in Fig. 1.

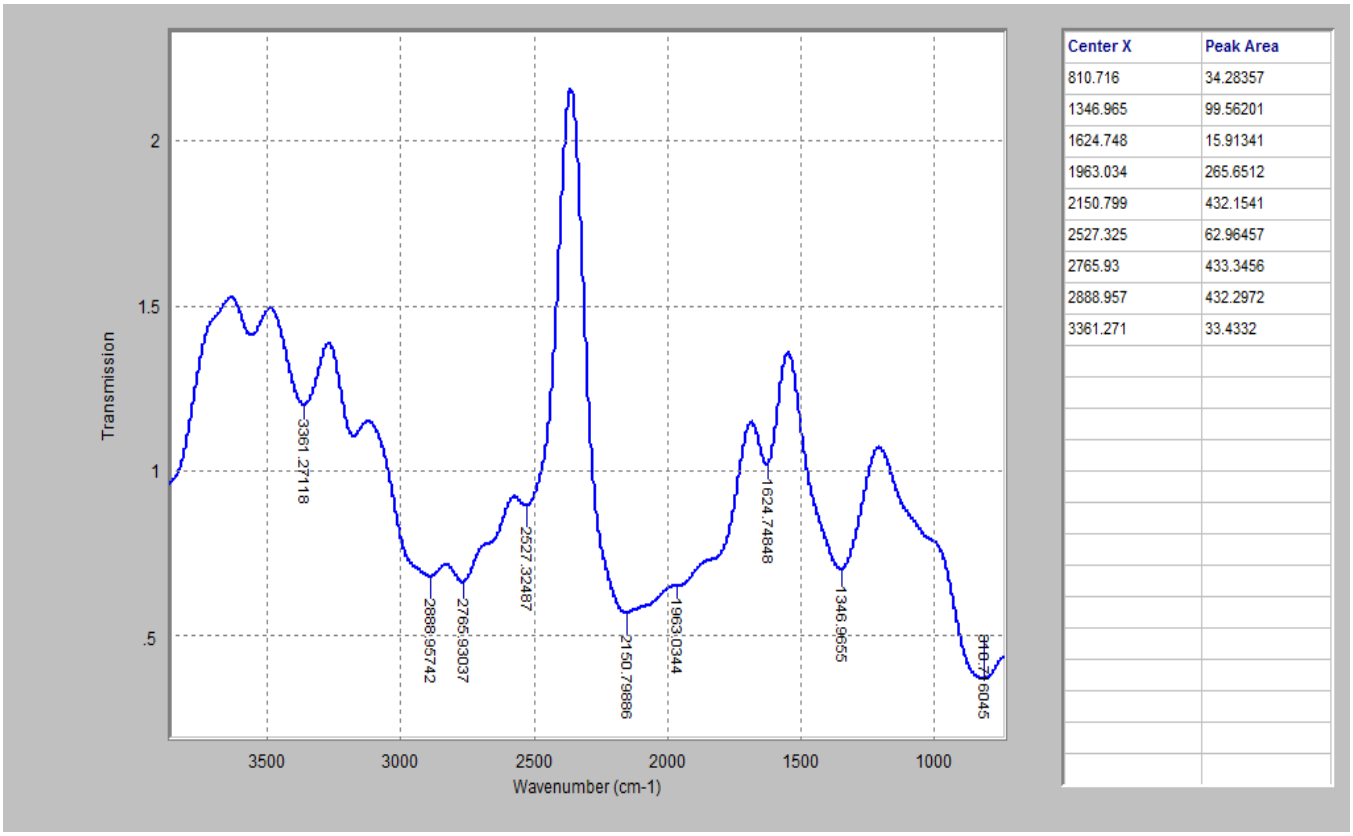

Center X	Peak Area
810.716	34.28357
1346.965	99.56201
1624.748	15.91341
1963.034	265.6512
2150.799	432.1541
2527.325	62.96457
2765.93	433.3456
2888.957	432.2972
3361.271	33.4332

FIGURE 1: FTIR spectrum of fresh cow blood.

Fig.1 shows plots of infra-red transmittance against wave number for fresh cow blood. The Fourier Transform Infra-Red spectra presented were obtained to consider the possible outcome of the interaction between the functional groups. Functional groups were assigned to distinct peaks as shown in the figure.

From Fig.1 representing the fresh cow blood sample, the peak of 816.716cm^{-1} was assigned to C-CI stretching vibration of Chloro compound. The absorbance of 1348.966cm^{-1} was assigned C=C stretching vibration of ethene compound. The medium band at 1624.746cm^{-1} was assigned to NH stretching vibration of 1^{o} amine compound. The wavelength around 1963.034cm^{-1} was assigned to SCN anti-symmetric stretching vibration of thiocyanate compound. The absorbance around 2150.799cm^{-1} was assigned to CO stretching vibration of carboxylic acid. The peak around 2527.325cm^{-1}was assigned to CN anti-symmetric stretch of nitrile compound. The weak bands around 2765.930cm^{-1} and 2866.957cm^{-1} were both assigned to CH stretching vibration of methylene compound respectively. The strong band around 3361.271cm^{-1} was assigned to OH stretching vibration of 2^{o} alcoholic compound.

It can be deduced that the fresh bull blood sample has more chloro compounds and also contains alkenes with moderate band. The amine compound (NH) responsible for proteins changes bond length, this goes to show that the protein in the fresh cow blood is not digestible (Donkoh *et al.*, 1999). The Thiocyanate compound in the fresh cow blood sample has one of the bonds increasing and the other decreasing showing its instability and underscoring the inedibility of the fresh cow blood. The fresh cow blood sample has traces (small amount) of carboxylic acid and nitrile compounds. The higher the wavelength, the lower the frequency of compounds. The least compound in the fresh cow sample is the alcoholic compound. The presence of Hydroxyl group goes to emphasize the presence of water molecules in the fresh cow blood sample.

III. CHARACTERIZATION OF COW BLOODMEAL

Based on the proximate analysis carried out by Bari, *et al*. (2015) on bloodmeal. Bloodmeal will be useful and effective in livestock feed formulation and other agricultural purposes. The chemical composition of convective oven dried bloodmeal showed that it contained more ash, fat, protein, carbohydrate and fibre than the fresh cow blood sample. The fresh sample is only higher in moisture content. The values reported by National Research Council (NRC), (1994) tend to agree with the values presented here for the proximate composition. The results indicate a very high concentration of Carbohydrate and Protein in the convective oven dried bloodmeal. Donkoh *et al.* (1999) and Bari *et al*. (2015) posited that Bloodmeal contains

substantial amounts of essential (indispensable) amino acids. The difference in the proximate compositions of the fresh and dried samples can be attributed to the drying process. Processing of bloodmeal increases the nutrient contents and its digestibility. Overheating during drying of bloodmeal can substantially lower digestibility and availability of the nutrients in the product (Donkoh *et al*. 1999). This goes to say that the processing conditions used in the preparation of bloodmeal can adversely affect the nutritional quality of the product. Bari *et al*. (2015) recommended that Bloodmeal is hygroscopic and less than 10-12% db moisture is allowable to prevent it from deterioration.

IV. FOURIER TRANSFORM INFRA-RED SPECTROSCOPY OF BLOODMEAL

Results of FTIR spectra of the bloodmeal is recorded in Fig. 2. From the plot, the peak value of 889.9796cm^{-1} was assigned to C-CI stretching vibration of Chloro compound.

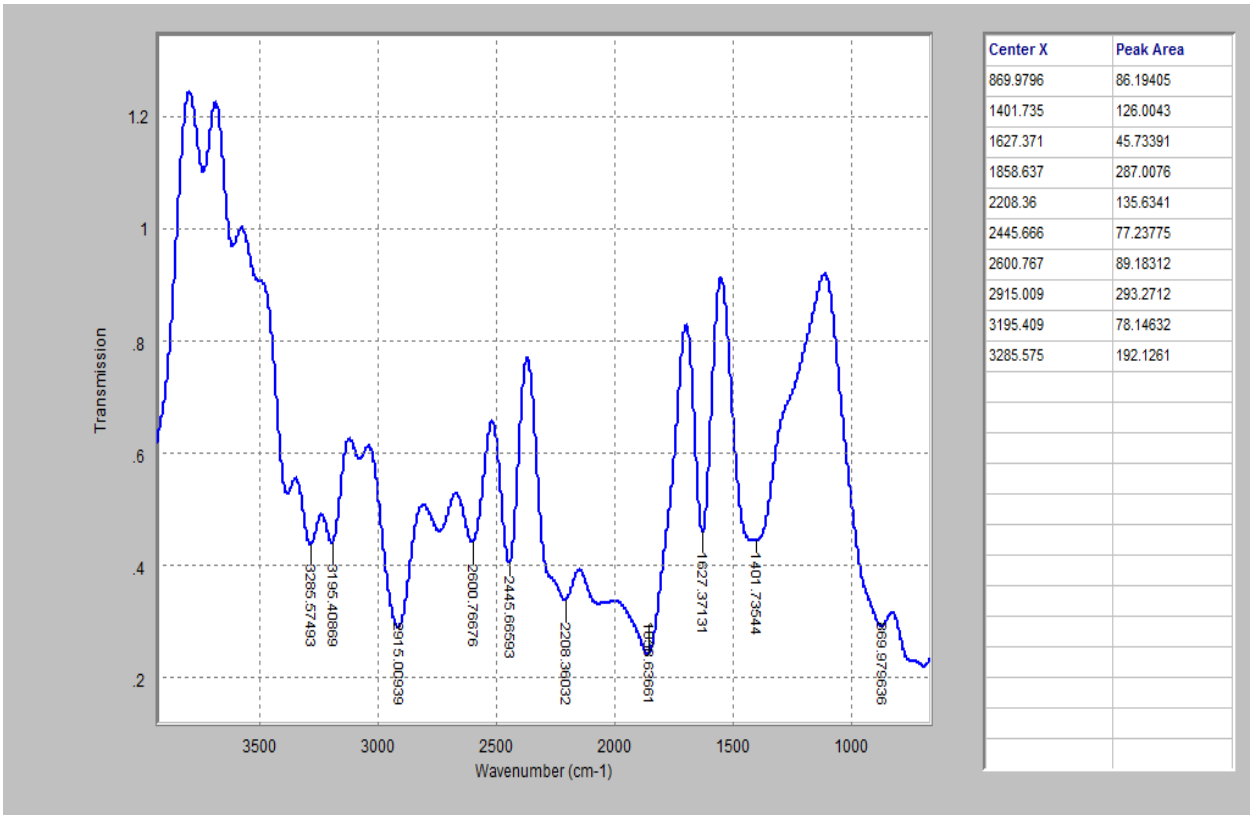

Center X	Peak Area
869.9796	86.19405
1401.735	126.0043
1627.371	45.73391
1858.637	287.0076
2208.36	135.6341
2445.666	77.23775
2600.767	89.18312
2915.009	293.2712
3195.409	78.14632
3285.575	192.1261

FIGURE 2: FTIR spectrum of bloodmeal.

The absorbance around 1401.735cm^{-1} was assigned C=C stretching vibration of ethene. The peak value around 1627.371cm^{-1} was assigned to NH stretching vibration of 1^{o} amine compound. The wavelength around 1858.637cm^{-1} was due to CO stretching vibration of cyclic ester compound. The peak around 2208.360cm^{-1} was assigned to CO anti-symmetric stretch of carbonyl compound whereas the band around 2445.666cm^{-1} was assigned to CN anti-symmetric stretch of nitrile compound. The weak band around 2600.767cm^{-1} was assigned to CH symmetric vibration of methylene compound. The value at 2915.009cm^{-1} was assigned to SCN stretching vibration of thiocyanate compound. The broad band around 3195.409cm^{-1} and 3285.575cm^{-1} were both assigned to OH stretching vibration of 1^{0} alcohol respectively.

The changes observed in the spectra represent interactive effects due to the functional groups during drying (Fig. 2); thus, some modifications are likely to have occurred. There are glaring differences in the Fourier transform infra-red spectroscopy of the fresh blood sample (Fig.1) and dried blood (bloodmeal) sample (Fig. 2). Different peaks were assigned to the Chloro compound in the two samples even though the two samples contain more chlorine compounds. The dry sample has a higher peak of Chlorine compounds; this shows that there is more in the number of chlorine compounds in the fresh sample than in the dried sample. The absence of the vibration in the amine (NH) compound in the dried sample underscores the availability of proteins in bloodmeal and its digestibility in the dried form (Donkoh, *et al*., 1999). The bloodmeal still contained traces of water. The Carboxylic acid and Cyanide are contained in the bloodmeal at a very negligible quantity.

The results also showed that some peaks were shifted from what they were in fresh blood. Some peaks even disappeared while new peaks were detected. These changes observed in the spectra show the interactive effects due to involvement of those functional groups during drying.

REFERENCES

[1] Bari, Z.A.; Hossain, M.A.; Alamgir, M. and Maref, M.U. (2015). An entire Process for the Isolation of Bloodmeal from Animal Blood and Microbial Investigation in Bloodmeal. Journal of Agriculture and Veterinary Science. 8(2): 42-46.

[2] Damba, C. (2017). Effects of Drying conditions on protein properties of bloodmeal. http://researchcommons.waikato.ac.nz/

[3] Davila Ribot, E. (2007). Advances in animal blood processing: development of bio preservation system and insights on the functional properties of plasma. Doctoral dissertation, PhD thesis, Universidad de Girona, ISEN 978-84-690-5988-3.

[4] Donkoh, A., Atuahene, C.C., Anang, D.M. and Ofori, S.K. (1999). Chemical Composition of Solar-dried bloodmeal and its effect on performance of broiler chickens. Journal of Animal Feed Science and Technology, 81:299-307.

[5] Hsieh, Y.; and Ofori, J.A. (2011). Food grade proteins from animals' byproducts: Their usage and detection methods. CRC press. New York, NY, USA.

[6] National Research Council (1994). Nutrient Requirement of Domestic Animals. Nutrient Requirements of poultry, 9th revised ed., National Academy Press, Washington, DC., USA.

Gas Analysis Codivirus Method for Detecting the Threshold of Contagiousness and Therapy Adjustment

Vlastopulo.V.I.[1*], Chaadaev. I. E.[2], Gazin.A.V.[3]

[1]Biophysical Department, Research Institute of Life and Ecology, Odessa, Ukraine
*Corresponding Author

Received: 24 April 2022/ Revised: 08 May 2022/ Accepted: 16 May 2022/ Published: 31-05-2022

Abstract— *To date, there is no easy-to-use method and device for its implementation for the detection of codivirus-infectious people by exhalation. The main method of covid infection is airborne when droplets of the infected saliva person enter the oral cavity of healthy person. Such method would make it possible to detect infected people and prevent them from entering in public places and send them to quarantine immediately. The method is not traumatic, unlike the PCR test, and along with other methods, it would allow adjusting the patients covid treatment in the hospital. Currently, gas analyzers are accurate research methods with a division value of 1 ppm. The purpose of this work is to identify which gases during the exhalation of infected or sick person are decisive, how to measure them during exhalation, how these gases are associated with entry proteins and enzymes of saliva? How change a gas concentrations depending from the infection and illness time, and what are their values?.*

Keywords— codivirus-infectious people by exhalation, gas analyzers.

I. INTRODUCTION

The main route of covid infection is aerosolized saliva from person's mouth into mouth. Droplets are formed as result of coughing, sneezing or conversation [1,2].

Till three thousand infected small droplets are formed at coughing. Almost the same numbers of droplets are formed during 5-minute conversation [3]. A single sneeze produces up to 40,000 droplets of saliva with different dispersion to some meters [3]. Normal exhalation produces droplets of saliva that can be airborne up to 1 meter. Larger and heavier droplets of saliva tend to fall to the ground by ballistic trajectory. Small cloud droplets are formed and then with air currents are transported over longer distances [2,3]. Aerosols are solid particles suspended liquid in the air with ranging in size from 0.001 to 100 microns [3]. The time the droplets remain in the air travel depend from their size [3]. Large droplets (diameter > 60 μm) tend to settle quickly. Transmission via small droplets (diameter ≤ 60 μm) can occur over short distances (distance between people less than 1 m). There is possibility also that small droplets under favorable conditions will turn into airborne suspension of infectious particles (diameter <10 μm) and carried over longer distances [4].

In other words, oral cavity this is initial place of covid infection.

On the other hand, in the study of human venous blood was found that the concentrations of carbon dioxide and bicarbonates increase significantly, by 83% and 8.8%, respectively [5].

Besides, during covid infection observe for more half of sick persons a dry mouth and amblygestia (a dulling of the sense of taste). These symptoms arise from impaired tongue function from ACE2 expressing and furin and also ACE2 expression in the salivary glands [6].

Currently, there are gas analyzers for determining the concentration of gases with division value of 1 ppm or 0.000001 fractions in air. That's why it is technically possible to detect changing of the carbon dioxide and hydrocarbonate suspension concentrations in the air at covid contagiousness people at exhale for distance till 1 meter.

II. PROBLEM FORMULATION

The technical task of this work was to create a gas analyzer with calibration for carbon dioxide and for suspended saliva hydrocarbons in the air based on the Arduino microcontroller with digital signal processing and comparing the results with calibration curves by this gases, with follow visualization of these changes on the screen, sensor buzzer and telegram channel messenger with a division value of 1 ppm. Research tasks are:

1. Is there an increasing of carbon dioxide and suspended saliva bicarbonates concentrations during human exhalation of infected covid patients and what is their percentage ratio?
2. How change the concentrations of carbon dioxide and saliva bicarbonates suspension at exhales person from day time illness?
3. How are change the carbon dioxide and saliva bicarbonate suspension concentrations related with two key input proteins known as the ACE2 receptor and the TMPRSS2 enzyme?

III. RESULTS AND DISCUSSION

The gas analyzer has the following view

FIGURE 1: Gas analyzer

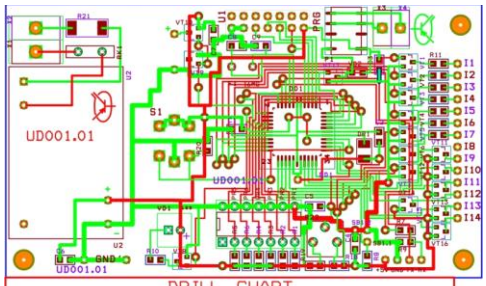

DRILL CHART

SYM	DIAM	TOL	QTY	NOTE
○	0.712 mm		50	
⊞	0.786 mm		2	
+	0.862 mm		18	
×	0.964 mm		44	
⌖	1.016 mm		3	
⊠	1.498 mm		6	
▵	1.600 mm		2	
◇	2.158 mm		2	
+	3.500 mm		3	
TOTAL			130	

FIGURE 2: Gas analyzer plata

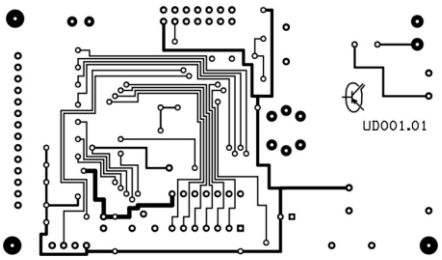

FIGURE 3: Gas analyzer plata-bot

The device was calibrated for carbon dioxide and saliva bicarbonates suspension at 20 degrees Celsius at normal atmospheric pressure and humidity with pre-treatment by bactericidal lamp. Data gas concentrations were measured by 1 or 2 analog gas detectors of the arrays data concentrations carbon dioxide P1 extensional and saliva bicarbonates suspension P2 extensional for nonequilibrium measurement system with follow by comparison arrays data calibration curves functional E1 , sub functional E2 both gases and with subsequent recording of nonlinear equations but already an equilibrium system

measurements with interactions of both gases during exhalation in a mixture of atmospheric air and then followed by digitization on Arduino microcontroller [7-9].

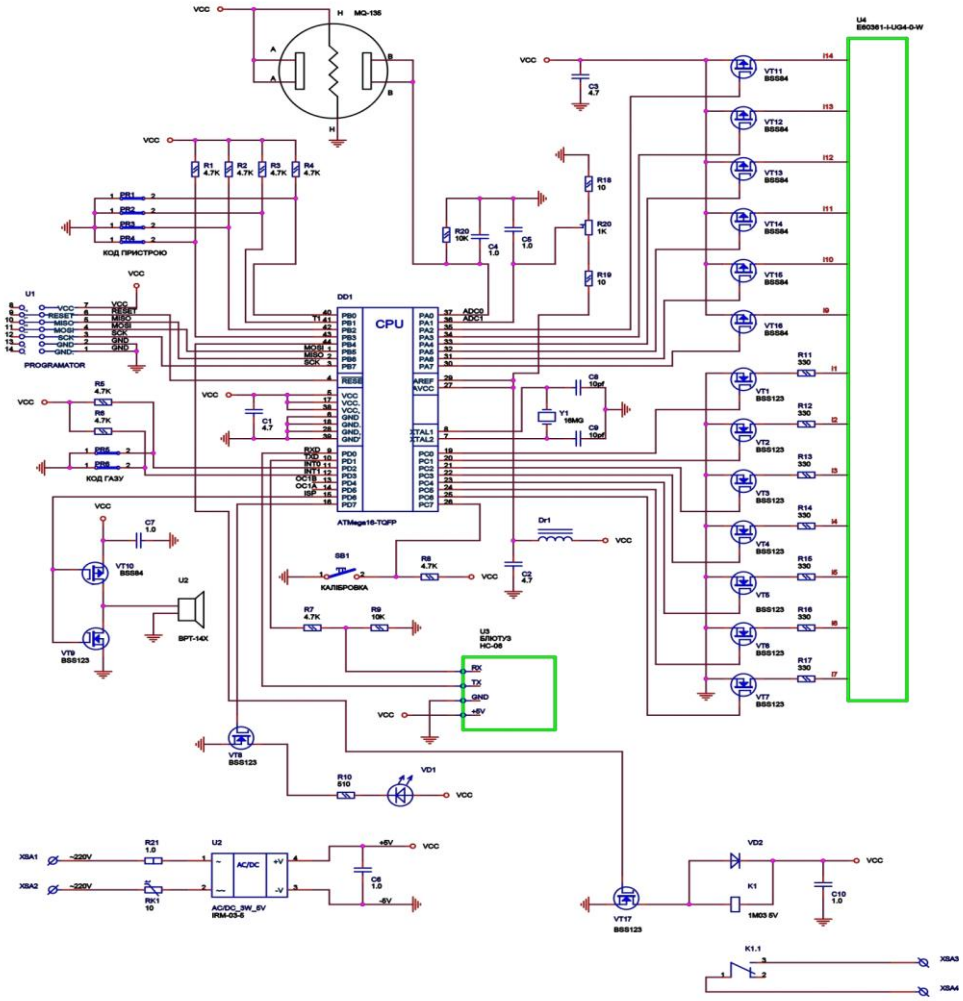

FIGURE 4: Gas analyzer scheme.

Analog signals are fed to the microcontroller. Below is a calculation of carbon dioxide concentration in air based on the calibration, experimental sensor resistance values, calculated analog-to-digital converter characteristics and the carbon dioxide value in air of the Global Atmospheric Bulletin for January 2022

$$Res/E_1 \times E_2 = [(adc_0 \times 0{,}1875/1000) \times 4 \times R_{load}] /E_1 \times E_2 \quad (1)$$

$$p = (Res/E_1 \times E_2) /ATM_{0CO2} \quad (2)$$

Res - detector resistance in Om,

E_1 - temperature correction coefficient,

E_2 - humidity correction coefficient,

$Res/E_1 \times E_2$ - calculate concentration carbon dioxide value in resistance detector units,

adc_0 - analog detector value,

U=float (adc_0) x 0,1875/1000, converting an analog detector value in voltage,

Coef V = 0.1875, constant for the accuracy of the analog-to-digital converter,

d = 1000, divisor to get value in volts,

Res = U x 5 - 1, here a resistance detector calculation,

V = 4 V, 4 volt gas analyzer supply,

R_{load} - resistor value in Om,

p - Carbon dioxide concentration in air in ppm,

ATM_{0CO2} = 417,99 ppm, carbon dioxide value in air in ppm at Global Atmosteric Bulletin, January, 2022. http//www.co2.earth/

Exactly the same calculation and for saliva bicarbonates concentration.

$ATM_{bicarbonates}$ = 16, 4 ppm , saliva bicarbonates concentration in air at health human exhalation defined by sampling of spectrophotometer Lambda 365, USA. Controlled also saliva samples of health and covid infected peoples and received a results 8-9,5 % in side of increasing, which is consistent with [5].

Calibration curves were built taking into account the temperature E_1 and humidity E_2 Winter-Summer regime at the Odessa latitudes and climate, Ukraine. To do this arranges a separate unit with temperature and humidity sensors into detector sheme. Other words, calculation coefficients ATM_{0CO2} = 417,99 ppm and $ATM_{bicarbonates}$ = 16, 4 ppm enter 1 time after calibration curves built on experimental values of temperature and humidity detectors.

Their changes show the intensity for each concentration relationship and for 2 functional or their sub functional have the form:

$$P_1 = f_1(E_1, E_2)$$
$$P_2 = f_2(E_1, E_2) \quad (3)$$

Fig. 5,6.

Differentiating among the equation, absolutely the outcome will be:

$$dP_1 = A_{11}\, dE_1 + A_{11} d\, E_2$$
$$dP_2 = A_{12}\, dE_1 + A_{12} d\, E_2 \quad (4)$$

The state coefficient nonequilibrium measure system A connects the functional and intensials, when changing from one nonequilibrium state to another, coefficients A temperature and humidity changes. Obviously, the coefficient of state is also a show the carbon dioxide and saliva bicarbonates concentrations E_2 of exhaled gases in the structure volumes of atmospheric air.

There are simple and cross-sectional coefficients of connections between singles structures of state and interactions of structures under distribution of exhaled gases in the volume of atmospheric air distributions. Basic and cross coefficients A in the form of corresponding functions of various functional E, as for carbon dioxide can be outdoor wind speed, the presence of cars and air pollution with carbon monoxide; for saliva bicarbonates concentrations this can be also outdoor wind speed and the presence of detergents based on soda or soda drinks :

$$A_{11} = f_{11}(E_1, E_2)$$
$$A_{12} = f_{12}(E_1, E_2)$$
$$A_{21} = f_{21}(E_1, E_2)$$
$$A_{22} = f_{22}(E_1, E_2) \quad (5)$$

We studied about 5,000 people with and without signs of covid in the street, quarantine and hospitals. The subjects exhaled air with open mouth for distance 10 cm. The values of gas concentrations were recorded on the display. Research has identified the following groups of people: 1. Healthy people who haven't any covid external signs and both gas concentrations no increase. 2. Healthy (infected -?) people who haven't any covid external signs of the disease, but have elevated concentrations of either carbon dioxide or both gases, possibly an asymptomatic form. 3. Infected people who have external signs of illness and have elevated concentrations of either carbon dioxide or both gases. 4. Sick people who have external signs of illness and have more elevated concentrations of both gases. 5. Sick people who have external signs of the disease, but recovering and having elevated concentrations of either carbon dioxide or both gases with tendency to decreasing.

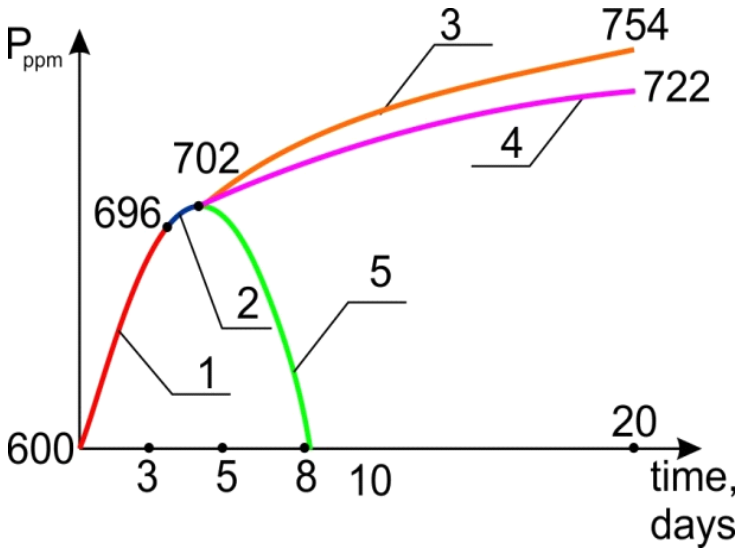

FIGURE 5: Curve of concentrations of carbon dioxide during exhalation of infected and sick people with covid.

The results of the research are presented by graphs of carbon dioxide concentrations (Fig.5) and suspensions of bicarbonates in saliva (Fig. 6) depending from infection day at exhalation. The counting of the curves is considered from start of infection for given room with values 630 and 35 ppm concentrations of carbon dioxide and suspended bicarbonates in saliva respectively. Curve 1 (red colour) is the area of infection with increasing of gas concentrations to 696 and 39 ppm of carbon dioxide and suspended bicarbonates respectively and corresponds to groups 2 and 3 of asymptomatic and infected people. Curve 2 (blue colour) is the area of disease stabilization with slight increases of gas concentrations to 702 and 40 ppm of carbon dioxide and suspended bicarbonates respectively.

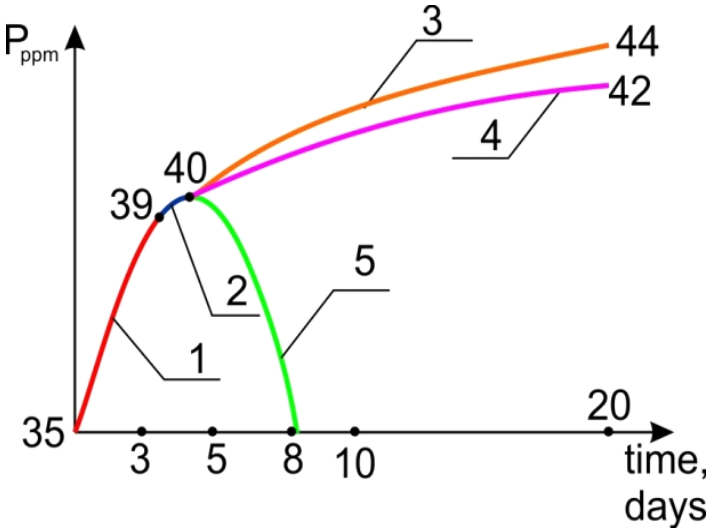

FIGURE 6: Curve of concentrations of suspension of bicarbonates in saliva during exhalation of infected and sick people with covid.

Curve 3 (orange colour) is a further escalation of the disease with increasing of concentrations to 722 and 42 ppm of carbon dioxide and suspended bicarbonates respectively and correspond to medium form of severity of covid illness. Curve 4 (crimson colour) is a further escalation of the disease with increasing of concentrations to 754 and 44 ppm of carbon dioxide and suspended bicarbonates respectively and correspond to heavy form of severity of covid illness. Curve 5 (green colour) show a recovery of human and decreasing a value both gas concentrations. The gas analyzer examines the process of infection through saliva in the oral cavity. If we consider curves 1 and 2 from the side of key entry proteins ACE2 receptor and the TMPRSS2 enzyme we can approve about infection development (Fig.5,6) [5], curve 2 as blocking the infection development in the body host human with codivirus colony. It correspond a results many researchers that 2-3 days after the

first disease signs appear dry mouth and decrease the saliva production. Covid disease seems to spread to the bronchi and lungs.

IV. CONCLUSION

It is possible to detect covid illnesses by gas analyzers based on person's exhalation. Carbon dioxide and a suspension of bicarbonates in saliva show a steady increasing to 150 and 20 ppm respectively. Both curves are characterized by the stage of infection, a sharp increasing in the concentrations of both gases from the first hours to 2-3 days of illness depending from different strains. Further, the disease stabilizes within 1-2 days. After that covid illness passes in medium or heavy form or the person recovers.

ACKNOWLEDGEMENTS

I thank the editors of the Journal for their help and publication of this paper. Special thanks to my teacher prof. Alfred Veinik for the selection of my research in the thermodynamics of nonequilibrium systems in nature and research technologies.

REFERENCES

[1] https://www.who.int/news-room/q-a-detail/q-a-coronaviruses#.

[2] Kohn, W. G. et al. Guidelines for infection control in dental health-care settings-2003. MMWR Recomm. Rep. 52, 1–61 (2003).

[3] Tang, J. W., Li, Y., Eames, I., Chan, P. K. & Ridgway, G. L. Factors involved in the aerosol transmission of infection and control of ventilation in healthcare premises. J. Hosp. Infect. 64, 100–114 (2006).

[4] Fennelly, K. P. et al. Cough-generated aerosols of Mycobacterium tuberculosis: a new method to study infectiousness. Am. J. Respir. Crit. Care Med. 169, 604–609.

[5] Dzemal Elezagic, Wibke Johannis, Volker Burst, Florian Klein and Thomas Streichert. Venous blood gas analysis in patients with COVID-19 symptoms in the early assessment of virus positivity. From the journal Journal of Laboratory Medicine/. https://doi.org/10.1515/labmed-2020-0126

[6] Chen, L. et al. Detection of 2019-nCoV in Saliva and Characterization of Oral Symptoms in COVID-19 Patients. https://ssrn.com/abstract=3557140 (2020).

[7] Vlastopulos Vladyslav, Plenary Lecture 2: «Creation of Electromagnetic Structure-Creating Spaces to Improve the Growth of Some Types of Cells and Albumins». Recent Advances in Biology, Biophysics, Bioengineering and Computational Chemistry Proceedings of the 5th WSEAS international conference on CELLULAR and MOLECULAR BIOLOGY, BIOPHYSICS and BIOENGINEERING (BIO'09) ISBN: 978-960-474-141-0, ISSN: 1790-5125

[8] Vlastopulos V.I., Nikolaev V.G., Bioenergetic fields of the human brain rhythmus. The using in video, audio products for the creating attracted bioenergetic advertisement, article №9B1840, materials of conference EBSA2009, conducted since 11 to 15 July in Genoa, Italy, 2009.

[9] Equations of Thermodinamics for Expansion and Filling by Human Civilization. Vlastopulo.V.I.[1], Polichronidi.A.G[2] IJ0ER-2021-N0V-1.

Cost-Effective Replacement Decision for the Transmission Unit of Locally Fabricated Palm NUT Digester

D. O. Ikeogu[1], D. O. Amaefule[2*], C. O. Nwajinka[3], V. M. Mbachu[4]

[1]Department of Vocational Education, Federal College of Education (Technical, Umunze, Anambra State
[2,3]Department of Agricultural and Bioresources Engineering, Nnamdi Azikiwe University, Awka, Anambra State
[4]Department of Industrial and Production Engineering, Nnamdi Azikiwe University, Awka, Anambra State
*Corresponding Author

Received: 18 April 2022/ Revised: 04 May 2022/ Accepted: 10 May 2022/ Published: 31-05-2022

***Abstract*—** *This study sought to establish optimum techno-economic replacement policies for the transmission unit of locally-fabricated oil palm fruit digester for cost-effective operation over a planning horizon of sixteen years. Deterministic Dynamic programming models were used in the study. The companies whose records were most amenable to the model's application were used as as cases for the study. The records were painstakingly collated and processed for deployment in the models. The depreciation, cost of operation and maintenance, and the Equivalent Uniform Annual Cost (EUAC) of the unit were evaluated. The equipment EUAC is evaluated over all the periods of the planning horizon. The period with the lowest EUAC is recommended by the model as the most cost-effective replacement period. The companies' replacement practice was assessed for its conformity with the replacement policy predicted by the model in a kind auditing approach. The companies were shown to incur increased EUAC for retaining the transmission unit beyond the replacement age recommended by the models. Deployment of replacement models for machinery replacement decisions support can enhance an industry's economic advantage in today's competitive industrial environment.*

***Keywords*— Oil palm fruit digesters, Dynamic programming models, Equipment replacement age, Equipment economic life, Replacement practice audit and Equivalent uniform annual cost.**

I. INTRODUCTION

Palm Oil is one of the commodities besides petroleum products that have contributed greatly to Nigerian economic survival, as Nigeria was the world's largest producer of palm oil then (Okafor, 2007). There is great economic problem in Nigeria today, and a dire need of diversifying the economy (Okafor *et al.*, 2010). Resuscitating the agricultural sector; the oil palm production sub-sector inclusive, is a welcome idea. During the era of palm oil production boom in Nigeria, crude technologies were deployed; with the traditional techniques dominating most of the production lines. Little maintenance cost was incurred with these technologies due to the associated minimal wear and breakdown. The growing world population and recent emphasis on renewable energy have led to increased demand on palm oil production and the need of advanced technologies for its production.

Modern oil milling today employs palm fruit digesting and mashed fruit oil-expressing machines, most of which have high wears and breakdown in their power transmission units and material-processing screws. While the digesting and oil pressing units of these machines are fabricated locally, their power transmission units which have gear transmission systems are imported. As a result, foreign exchange is incurred in the procurement of these gear transmission units. Studies on their maintenance and replacement costs dynamics will assist in profitable management of our local oil mills. Premature retirement of equipment results in underutilization and consequently waste of resources and poor productivity. On the other hand, retaining the equipment beyond the useful economic life leads to incurring the avoidable higher cost of running and maintaining the parts or machine. This has a negative effect on the overall productivity of the system. The optimum replacement plan or time of the palm fruit digesting and mashed fruit oil-expressing screw presses' gear transmission units depends on the economic life of the units.

Few studies on agricultural processing equipment's costs and economics have been carried out in the country. Oluka and Nwani (2013) studied the repair and maintenance costs of rice mills and developed a model for estimating the maintenance cost in Nigeria. Nwajinka (2010) developed computer-assisted methods for predicting the optimal-cost size and replacement time for farm tractor. Amaefule *et al.* (2018a) developed a minimum-cost model for selecting tillage machinery for combined use of farmers. Grano and Abensur (2017) reported that there are limited studies on the application of industrial assets replacement policies to farm equipment. Bagshaw (2017) presented maintenance and replacement scenario and costing encountered in manufacturing setups.Studies on the maintenance and replacement costs dynamics of the gear transmission units will assist in profitable management of our local oil mills. Deploying machinery replacement models in arriving at the most economic time for the replacement of oil palm fruit digester gear transmission units is needed for profitable oil palm milling. This work is aimed at establishing policies for the economic replacement of locally fabricated palm fruit digester transmission unit.

II. MATERIALS AND METHODS

2.1 Theoretical Considerations

In equipment replacement problems, the equipment in service that is considered for replacement (the defender) must have a better challenger (the considered alternative equipment) for the replacement to be worthwhile. The challenger and defender can equally be a unit of the equipment when what is considered for replacement is only the unit. Service life, accounting life and economic life are 3 concepts of machine life (Hunt and Wilson, 2015). Equipment economic life is the period of time the equipment can be retained in service without resulting in adverse equipment cost arising out of uneconomic repair cost or obsolescence. While the technical competence must necessarily be considered in machine replacement, the economics of the machine and in particular the involved costs and returns are easily employed in the machine replacement modeling (Zvipore *et al.*, 2015). The trade-in value of the defender is treated as a reduction in the initial cost of the challenger (Li, 2015).

Investment receipts and disbursements are regarded as cash inflows and cash outflows respectively. By convention, financial transactions made during a period are assumed to occur at the end of the period, for ease of investment problems articulation. The replacement planning horizon covers the period from the point of replacement decision to the end of the service life of the challenger. Abensur (2010) stated that an equipment trade-in value should include its cash flow beyond the planning horizon if its working life is greater than the service life. Variable machinery costs vary directly as the machinery use and can be expressed on hourly basis, or as cost per unit output or other appropriate measures (Field and Solie, 2007 and Amaefule *et al.*, 2018b). Energy, oil, lubricants, labour and repair and maintenance costs are classed as variable costs.

In replacement analysis the average annual cost (*AC)* of the defender is compared with that of the challenger in evaluating the replacement period. For each decision period *i* of the *n* years of the equipment life, the *AC* of owning the equipment up to period *i* is obtained for the challenger and defender. The *AC* of purchase cost (*P*) for the period *i*, is added to the operating cost (C(i)) in the same period, while the resale value (*S)* at the periodis subtracted from the sum for the equipment. The replacement period which gives the minimum total *AC* of the challenger is its economic replacement age, *i.e.* the challenger's optimum economic life (Bagshaw, 2017). The equivalent annual cost (*EAC*) is evaluated by reckoning the time value of the involved cash flows using the appropriate interest rate (*r*) and discounting period (i), as shown in equation 1 and 2.

$$EAC = P\left(A/P_{r,i}\right) + C(i)\left(A/P_{r,i}\right) - S\left(A/F_{r,i}\right) \quad (1)$$

$$EAC = (P + C(i))\left(A/P_{r,i}\right) - S\left(A/P_{r,i}\right)\left(P/F_{r,i}\right) \quad (2)$$

2.2 Equipment Replacement Modelling

The average annual cost (*AC*) of the machine is obtained by dividing the total concerned cost with the estimated machine life. The model employs the operation, maintenance and equipment ownership costs, and the equipment economic life in estimating the annual cost (Sharma*et al.*, 2006 and Tayari, 2018). In evaluating their Equivalent Uniform Annual Cost (*EUAC*) the time values of the involved costs are incorporated into the replacement model (Grano and Abensur, 2017). Machinery costs that remains unchanged for both the defender and challenger; such as is more likely in like-for-like replacement, are overlooked (Sharma and Sharma, 2007 and Hunt, 1999). Only the costs that vary are considered in the operating cost.

A Dynamic Programming (DP) replacement decision support procedure for a machine that deteriorates with age following total cost minimization approach was developed by Li (2015). Based on it the following assumptions applicable to the case under review were made:

a) Machine will be owned during each of the *n* year periods.

b) The age of the (defender) machine when we start the process (replacement decision) process is known and denoted as y.

c) Known annual operating cost of machine aged *i* yrs (which) at the start of the year is and is given as $C(i)$.

d) Price of the new machine (the challenger at age 0) is known and denoted as P.

e) Known trade-in value $t(i)$ for a machine aged i years at the start of the year.

f) Known salvage values (i) for the i years aged machine at the end of year n.

The objective of the DP problem was the minimization of $[S(x; k)]$; the cost of owning a machine for the years k to n; which is the planning horizon.

The age of the challenger is x years at the start of year $x: k$;

$k = 1, 2, \dots, n$

$x = 1, 2, \dots, k-1, y+k-1$ when $k > 1$

and

$x = y$ when $k = 1$

The generalized form of the DP model was as shown in Equation 3

$$S(x: k) = min\{\underset{KEEP}{\overset{REPLACE}{\Longrightarrow} p - t(x) + c(0) + S(1{:}k+1)} \atop \Longrightarrow c(x) + S(x+1{:}k+1) \quad (3)$$

DP Interpretation

The optimal value of the objective was to minimize $S(x; k)$ the cost of owning a machine from year $\boldsymbol{k}$ through $\boldsymbol{n}$; starting the year $\boldsymbol{k}$ with a machine that just turned age $\boldsymbol{x}$, for $k = 1,2, \dots, n$ (Zvipore *et al.*, 2015).

The policy from this optimal function will translate to:

$P(x; k) = "REPLACE"$ if replace is cheaper than "$KEEP$" in the recursive relation, and

$P(x; k) = "KEEP"$ if otherwise.

The boundary condition being

$S(x; n+1) = -s(x)$ For $x = 1, 2, \dots, n$ and $y + n$

2.3 Study Area

Orumba South Local Government Area located within latitude 5.96778N – 6.0163N and longitude 7.14758E – 7.3166E, is one of the twenty-one (21) local governments in Anambra State, Nigeria. It lies within the oil palm belt of the rain forest zone of Nigeria. Major small-scale palm oil mills in the area were studied. The oil palm digesters studied were locally fabricated and are of the vertical type. They operated on rotary mechanism and were each powered by an 8 HP stationary diesel engine. The digesters had gear transmission systems made from rear wheel axles of Toyota Dyna trucks. Though the use period before importation could not be ascertained, the transmission units were regarded as good-as-new for replacement purposes in this study.

1 batch of the digester's process vessel (drum) held as much as 540 kg of palm nut. Breakdown maintenance of the transmission unit was practiced in the companies; and was done only when the unit failed. Operator's wages was a fixed

amount per drum plus 0.72 litres of palm oil per batch of the processed product. This could not amount to differences in labour costs in the defenders and challengers. The oil mills were visited to obtain the general information on the maintenance and replacement practices they carried out on their digesters power transmission units. The data from a representative was used, for analysis and modelling.

III. METHODOLOGY

Data used for this study were obtained from both primary and secondary sources. Primary field data were obtained from the oil mills visited. Secondary data were obtained from manufacturers' manuals, relevant handbooks on machine maintenance and published journals papers. Descriptive survey was adopted for this study research design. Diesel consumption was obtained from the company's record, while the unit cost was obtained from national statistical data. The purchase cost and the salvage values of the transmission unit were obtained from the company's records. Prices for the intermediate years when purchase of new unit or sale of the scrap unit did not occur were obtained by regression models. A kind of auditing approach was deployed in assessing the economic effectiveness of the companies' replacement practice vis a vis the recommendations of the replacement model for the unit.

IV. RESULT AND DISCUSSION

The replacement decisions given by the DP model for the transmission unit of the studied company for the years 1999 to 2006 is shown in Table 1. The replacement decision for each stage of the planning horizon is also shown. The *EUAC* and annual transmission unit cost are also shown. For year k=1, being 1999, the first year of installation and market value of the unit was ₦3,000.00. The unit was just installed and was not considered for replacement yet. In the year 2000, the market value was ₦2,120.00, the actual depreciation was ₦880.00, cost of capital value at 10% for beginning of the year (BoY) of market value was ₦300.00. Annual expenditure was ₦350.00, total (marginal) cost per year was ₦ 530.00, while *EUAC* was ₦1,530.00.

In this period under review; 2000, it was not due for replacement because the *EUAC* of the unit was less than that for the next year, but higher than that of previous year. Based on the model, replacement should be done when the *EUAC* is minimum. From Table 1, the unit was due for replacement at the end of 2003, but was not replaced by the company. It was rather repaired in 2004 and replaced in 2006.

TABLE 1
EUAC AND THE REPLACEMENT DECISIONS FOR 1999 TO 2006

End of Year (k)	Market Value @ End of yr k (₦)	Depreciation During yr k (₦)	*Cost of Capital (₦)	Annual Exp. (₦)	Total (Marginal) Cost per Year (₦)	EUAC for yr k (₦)	Replacement Decisions based on the model	Actual replacement decision
1999	3000						Starting point	
2000	2120	880	300	350	1530	1530	**Keep**	**Kept**
2001	1460	660	212	700	1572	1551	**Keep**	**Kept**
2002	1020	440	146	950	1536	1546	**Keep**	**Kept**
2003	800	220	102	1100	1422	1066	**Due For Replacement**	**Kept**
2004	2550	0	80	2600	2680	1388	**Overdue For Replacement**	**Repaired**
2005	1450	1100	255	1750	4555	1916	**Overdue For Replacement**	**Kept**
2006	600	850	145	1900	3495	2142	**Overdue For Replacement**	**Replaced**

cost of capital is 10% of Market Value @ BOY

The market value in the year 2004 was ₦2550.00, and the actual depreciation was ₦0.00; indicating that the unit have outlived its economic life. The cost of capital was ₦145.00, annual expenditure was ₦2,600.00, and total annual (marginal)

cost was ₦2680.00. *EUAC* increased to ₦1,388.80. It is noteworthy that in the period under review, based on the model's decision criteria, the unit was long overdue for replacement, since its *EUAC* has begun to increase after arriving at its minimum value in the previous year. In 2006, the market value was ₦600.00, the actual depreciation was ₦850.00 and cost of capital ₦145.00. Annual expenditure was ₦1,900.00, and total annual (marginal) cost was ₦2,895.00. *EUAC* increased to ₦1,675.00 showing the unit as overdue for replacement based on the model's criteria. The company eventually replaced the unit in this period.

The replacement decision recommendations from the DP model for the unit in the studied company for the years 2006 to 2011 is shown in Table 2. In 2006; the second unit's year of installation, market value of the unit was ₦8,000.00, the unit was not considered for replacement yet. In the year 2007, the market value was ₦6,166.67, the actual depreciation was ₦1,833.33, and cost of capital was ₦800.00. Annual expenditure was ₦2,500.00, total (marginal) cost per year was ₦5,133.33, *EUAC* was ₦5,133.33, and indicating the unit was not due for replacement.

TABLE 2
EUAC AND THE REPLACEMENT DECISIONS FOR 2006 TO 2011.

End of Year (k)	Market Value @ End of yr k (₦)	Depreciation During yr k (₦)	*Cost of Capital (₦)	Annual Exp. (₦)	Total (Marginal) Cost per Year (₦)	EUAC for yr k (₦)	Replacement Decisions based on the model	Actual replacement decision
2006	8000						Starting point	
2007	6166	1833	800	2500	5133	5133	**Keep**	**Kept**
2008	4700	1467	617	3000	5083	5110	**Keep**	**Kept**
2009	3600	1100	470	3500	5070	5098	**Keep**	**Kept**
2010	2867	733	360	3800	4893	5054	**Due for replacement**	**Kept**
2011	2500	367	287	5600	6253	5250	**Overdue for replacement**	**Replaced**

cost of capital is 10% of Market Value @ BOY

In 2008, the market value was ₦4,700.00, the actual depreciation was ₦1,466.67, cost of capital ₦616.67, annual expenditure ₦3,000.00, total (marginal) cost per year was ₦5,083.33, *EUAC* was ₦5,109.52, and in the period under review, it was not due for replacement. In the year 2009, the market value was ₦3,600.00, the actual depreciation was ₦1,100.00, and cost of capital value ₦470.00. Annual expenditure on the unit was ₦3,500.00, annual (marginal) cost was ₦5,070.00, *EUAC* was ₦5,097.58 and in the period under review, it was not due for replacement.

In 2010, the market value was ₦2,866.67, the actual depreciation was ₦733.33, and cost of capital ₦360.00. Annual expenditure was ₦3,800.00, total (marginal) cost per year was ₦4,893.33, and *EUAC*₦5,053.57. In the period under review, it was due for replacement because the *EUAC* of the unit was lower than that for the previous year, and also lower than that of next year but the company did not replace. The unit should have been replaced as the model recommended. In the year 2011, market value was ₦2,500.00, the actual depreciation was ₦366.67, cost of capital was ₦286.66. Annual expenditure was ₦5,600.00, total (marginal) cost per year was ₦6,253.33, *EUAC* was ₦5,250.00. In the period under review, it was overdue for replacement because the *EUAC* has started increasing after reaching a minimum value in the previous year. The unit was eventually replaced in this period.

The replacement decisions given by the DP model for the transmission unit of the studied company for the years 2011 to 2015 is shown in Table 3. In the year 2011, when another new transmission unit was installed, the market value was ₦12,000.00. The unit was just installed and not considered for replacement yet. In the year 2012, the market value was ₦9,200.00, the actual depreciation was ₦2,800.00, and the cost of capital (10% of market value @ BoY) ₦1,200.00. Annual expenditure of ₦3,500.00 was incurred, total annual (marginal) cost was ₦7,500.00, and *EUAC* was ₦7,500.00. In the reviewed period, the unit was not due for replacement because the *EUAC* of the unit was greater than that for the next year. The company also did not replace unit.

TABLE 3
EUAC AND THE REPLACEMENT DECISIONS FOR 2011 TO 2015

End of Year (k)	Market Value @ End of yr k (₦)	Depreciation During yr k (₦)	*Cost of Capital (₦)	Annual Exp. (₦)	Total (Marginal) Cost per Year (₦)	EUAC for yr k (₦)	Replacement Decisions based on the model	Actual replacement decision
2011	12000						Starting point	
2012	9200	2800	1200	3500	7500	7500	**Keep**	**Kept**
2013	7100	2100	920	4300	7320	7410	**Keep**	**Kept**
2014	5700	1400	710	5200	7310	7376	**Due for replacement**	**Kept**
2015	5000	700	570	6800	8070	7550	**Overdue for replacement**	**Kept**

cost of capital is 10% of Market Value @ BOY

For the year 2013 the market value was ₦7,100.00, the actual depreciation was ₦2,100.00 and their costs of capital was ₦920.00. Annual expenditure was ₦4,300.00, total annual (marginal) cost was ₦7,320.00, EUAC was ₦7,410.00, and for this period, the *EUAC* of the unit was higher than that for the previous year, though less than that of next year. The unit was therefore not due for replacement. In the year 2014, the market value was ₦5,700.00, there was an actual depreciation of ₦1,400.00, and cost of capital of ₦710.00. Annual expenditure was ₦5,200.00, total (marginal) cost per year was ₦7,310.00, and *EUAC*₦7,376.67. In the period under review, the unit was due for replacement because the *EUAC* was lower than that for both the previous and next years. The company did not however replace it. In the year 2015, the unit had a market value of ₦5,000.00, the actual depreciation was ₦700.00, and cost of capital value ₦570.000. There was an annual expenditure of ₦6,800.00. Total (marginal) cost for the year was ₦8,070.00, and *EUAC* was ₦7,500.00. The unit was already overdue for replacement during the period under review and was eventually replaced.

V. CONCLUSION

The company's replacement activity was in tandem with the recommendations of the replacement policy given by the model for some of the years studied. Thus the keeping of the unit in the years 2000, 2001 and 2002 during the first transmission unit use period tallied with the models recommendations. However the failure to replace the unit in 2003, up till 2005 was contrary to the models recommendation of "Due for replacement". If the company had replaced the unit in 2003, there would have been a savings of ₦322.00 *EUAC* in 2004, an additional savings of ₦528.00 in 2005 and an extra savings of ₦226.00 *EUAC* in 2006. Also during the second transmission unit use period the non-replacement of the unit in the years 2007, 2008 and 2009 was in tandem with the model's recommendation of "Keep". But in 2010 the continued retention of the unit in service when the model recommended "Due for replacement" led to the *EUAC* gaining an increase after reaching a minimum value. If the company had replaced the unit in 2010, it would have reaped a *EUAC* savings of ₦196.00 in 2011. Similarly the keeping of the unit in the years 2012 and 2013 during the third transmission unit use period was in tune with the model's recommendations of "Keep". The continued retention of the unit in 2014 and 2015, however was contrary to the models recommendation "due for replacement". The company would have gained a *EUAC* saving of ₦173.33 in 2011, if the unit was replaced in 2010. Zvipore *et al.* (2015) reported revenue increase from DP-based replacement analysis of a gold mine conveyor belt via replacement age determination. In conclusion, the use of engineering economic models, including replacement models for machinery management decisions support can enhance an industry's economic advantage in today's competitive industrial environment.

REFERENCES

[1] Abensur, E. O. (2010). Um modelo alternativo de otimização para a política de reposição de equipamentos. Sinergia, 11, 140-150. Optimization models applied to equipment replacement policy. Proceedings of The XVI International Conference On Industrial Engineering and Operations Management Sao Carlos, Brazil October 12-15 2010: 2-13

[2] Amaefule, D. O., Oluka S. I. and Nwuba E. I. U. (2018a). A field machinery capacity selection model for tillage operations in Nigeria. Journal of Engineering and Applied Sciences (JEAS) 14: 1-12.

[3] Amaefule, D. O., Oluka S. I. and Nwuba E. I. U. (2018b).Tillage Machinery Selection Model For combined non-contiguous farms. JEAS 14: 13-25.

[4] Bagshaw, K. B. (2017). A review and analysis of plant maintenance and replacement strategies of manufacturing firms in Nigeria.African Journal of Business Management. 11(2):17-26.

[5] Field, H. L. and Solie, J. B. (2007). Introduction to Agricultural Engineering Technology A Problem Solving Approach 3rd Edition. Springer Science+Business Media, NY.

[6] Grano, C. and Abensur, E. (2017). Optimization model for vehicle routing and equipment replacement in farm machinery. Journal of Brazilian Association of Agricultural Engineering 37(5): 987-993. DOI: 10.1590/1809-4430-eng.agric.v37n5p987-993/2017

[7] Hunt, D. R. (1999). Cost Analysis. CIGR Handbook of Agricultural Engineering 3: 574-584.

[8] Hunt, D. R. and Wilson, E. (2015). Farm Power and Machinery Management (15thEdition). Iowa State University Press. Ames.

[9] Li, P. (2015). Equipment Replacement Problems (Lecture 7) Operations Research and Logistics (MATH 3220). The Chinese University of Hong Kong FEB 2015

[10] Nwajinka, C. O. (2010). Computer-assisted Methods for Predicting the Optimal Size and Replacement Time for Farm Power and Machinery. A Seminar Presentation for Agricultural and Bioresources Engineering Seminar (ABE 801) to the Department of Agricultural and Bioresources Engineering Nnamdi Azikiwe University Awka Nigeria.

[11] Oluka, S.I. and Nwani S. I. (2013). Models for repair and maintenance costs of rice mills in southeastern states of Nigeria. Journal of Experimental Research. 1(1): 10-15. www.er-journal.com

[12] Okafor, B. (2007). Minimizing metal wear in screw presses in palm oil mills, Journal of Engineering and Applied Sciences 2(4): 680-682.

[13] Okafor, B. E., Odi-Oweib, S. and Akor, A. J. (2010). Using regression analysis to model wear in flights in palm oil mill press screws 48. The West Indian Journal of Engineering 32(l&2): 1-5.

[14] Sharma, S. K., Sharma, S. and Sharma, T. (2006). Industrial Engineering and Operations Management. S. K. Kataria and Sons, Delhi

[15] Sharma, S. D. and Sharma, S. (2007). Operations Research. Kedar Nathram Nath Sons, New Delhi.

[16] Tayari, F. (2018). Mutually Exclusive Projects with Unequal Life Geo-Resources Evaluation and Investment Analysis (EME 460). The Pennsylvania State University. https://www.e-education.psu.edu/eme460/syllabus.

[17] Zvipore, D. C., Nyamugure, P., Maposa, D. and Lesaona, M. (2015). Application of the equipment replacement dynamic programming model in conveyor belt replacement: case study of a gold mining company. Mediterranean Journal of Social Sciences 6(2): 606-612.

The Effects of Operating Parameters on the Geometry of a Measurement Section of a Pipeline

Mária Čarnogurská[1*], Miroslav Příhoda[2]

[1]Department of Power Engineering, Faculty of Mechanical Engineering, Technical University of Košice, 042 00 Košice, Slovak Republic

[2]Department of Thermal Engineering, Faculty of Materials Science and Technology, VSB –Technical University of Ostrava, 708 33 Ostrava-Poruba, Czech Republic

*Corresponding Author

Received: 26 April 2022/ Revised: 07 May 2022/ Accepted: 11 May 2022/ Published: 31-05-2022

Abstract— *This article deals with the effects of a temperature, pressure, gravity, pipe flanges and saddle supports of a measurement section of the pipeline on changes in the pipe geometry. The investigation was aimed, in particular, at examining changes in diameters of two pipeline sections relative to changes in their internal pressure, which ranged from 0 MPa to 6.0 MPa, and to changes in temperature, which ranged from 0 °C to 25 °C. As indicated by the results of a numerical simulation carried out within this research, a change in a diameter can be expressed most accurately if the effects of gravity, saddle supports and flanges are neglected. Changes in pipe diameters were examined merely as a function of changes in pressure and temperature. Gravity, flanges and saddle supports cause irregular pipe deformities that occur along the pipe circumference and length. These effects prevented identification of real values of changes in the pipe diameter on the measurement sections of the pipeline.*

Keywords— measurement pipe section, saddle supports, flanges, gravity.

I. INTRODUCTION

In investigation into changes in geometry of a measurement section of the pipeline, intended for natural gas transportation, two of the operating parameters play a significant role—a temperature and a pressure of transported gas. These two factors affect the pipe geometry, while their effects depend on particular combinations of pressure and temperature values; eventually, they determine a measured amount of transported gas. This article presents an analysis of the effects of pressure and temperature on the pipe geometry, which was carried out with four different pressure and four different temperature values. The results of the investigation are presented in the concluding section of the article in form of tables for two different types of pipes. Effects of pressure and temperature were evaluated using three calculation models while applying numerical methods: ProMechanika, ANSYS CFX and CosmosM [1-2]. The investigation was aimed at identifying the impact of identical boundary conditions on the results obtained by using the above listed software products. Another examined aspect was a possibility to apply simplified boundary conditions and their effects on the result.

The basic parameters of the investigated geometry, as well as other selected technical data adopted from the data sheets for the materials from which both measurement sections of the natural gas pipeline were made, are listed in Table 1.

TABLE 1
BASIC PARAMETERS OF INVESTIGATED PIPES

Name	Value	Units
Nominal dimensions of the pipe	1) 762 x 25.4 – 1,200 2) 790 x 19.0 – 1,200	mm
Pipe material	S355 JR – 11523.1	-
Highest operating temperature	+50	°C
Lowest operating temperature	0	°C
Welded joint coefficient	0.85	-
Ultimate tensile strength at t = 20–50 °C	470	MPa
Yield strength at t = 20–50 °C	355	MPa
Modulus of elasticity	2.06105	MPa
Poisson ratio	0.28	-
Mass density	$7.85 \cdot 10^{3}$	$kg \cdot m^{-3}$
Thermal expansion coefficient	$2.0 \cdot 10^{-6}$	K^{-1}
Thermal conductivity	52	$W \cdot m^{-1} \cdot K^{-1}$
Specific heat	512	$J \cdot kg^{-1} \cdot K^{-1}$

II. ANALYSIS MODEL

The created calculation model for both pipe types was based on their real geometries, and it was made using the numerical FEM (Finite Element Method) [3-4]. Both pipes were part of a measurement section of the natural gas pipeline at the border acceptance gas station in Veľké Kapušany, Slovakia. The calculation model was created for identical, 1,200 mm long pipe sections. Due to the fact that the pipe structure was symmetrical to three coordinate axes as to its geometry, and to one coordinate axis as to its loading (a gravity effect in the direction of y-axis), the calculation could only be made for one half of the geometry. For both pipe types, the calculations were made for the following calculation statuses:

1. Calculation Status 1: a pipe loaded by internal pressure p = 0 MPa; a temperature of 0, 15, 20 and 25 °C; gravity, saddle supports, and flanges being considered.
2. Calculation Status 2: a pipe loaded by internal pressure p = 5 MPa; a temperature of 0, 15, 20 and 25 °C; gravity, saddle supports, and flanges being considered.
3. Calculation Status 3: a pipe loaded by internal pressure p = 5.5 MPa; a temperature of 0, 15, 20 and 25 °C; gravity, saddle supports, and flanges being considered.
4. Calculation Status 4: a pipe loaded by internal pressure p = 6 MPa; a temperature of 0, 15, 20 and 25 °C; gravity, saddle supports, and flanges being considered.

The article presents the investigation into the pipe specified in Table I, designated as 1), with the dimensions 762 x 25.4 – 1,200. The results presented below correspond to Calculation Status 2, designated as 2), wherein a pressure was p = 5 MPa and a temperature was 20 °C. The pipe model was created at the 1:1 ratio and is plotted in Fig. 1. The pipeline together with

flanges and saddle supports on which it was placed formed a compact unit. In this particular status, the effects of gravity were taken into consideration.

In real conditions, the effects of saddle supports, flange joints and the pipe weight are interlinked, hence there were complications with calculating the values of the pipe diameter following the deformation. Deformities that occurred along the pipe circumference were not identical; pipe diameter values exhibited differences at individual points on the pipe. The most significant pipe deformity, in the above specified boundary conditions, was observed in the areas where the saddle supports were located (Fig. 2). The strain value was $\delta = 0.184$ mm. Therefore, in the next step of the investigation the effects of gravity were neglected. In this case again, a maximum strain of the pipe diameter was observed in the saddle support area (Fig. 3). However, its value was a bit lower ($\delta = 0.172$ mm)

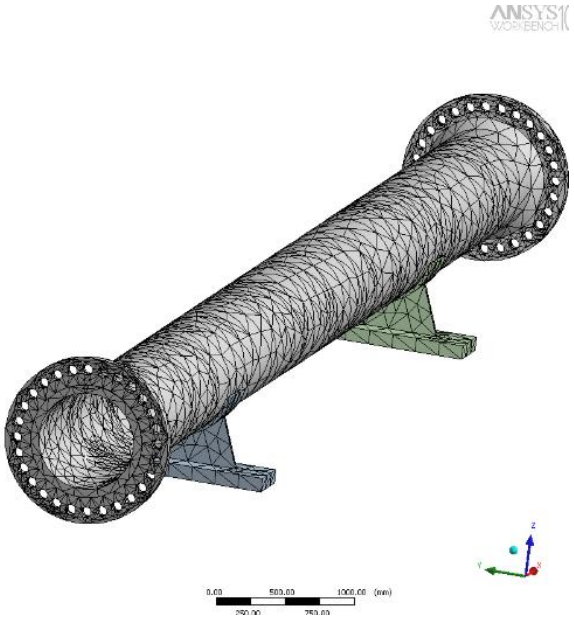

FIGURE 1: The pipe model

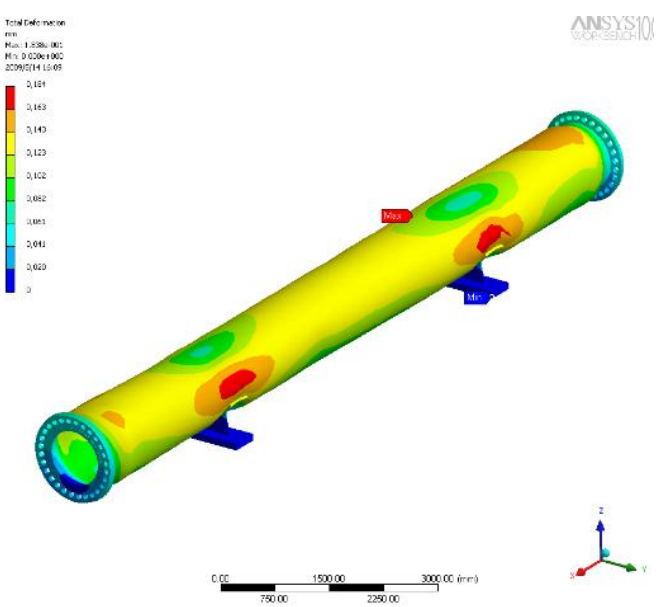

FIGURE 2: Pipe deformities, gravity being considered (p = 5 MPa; t = 20 °C)

It was decided not to consider flanges, saddle supports and gravity in determination of real changes in the pipe diameter. Hence, the examination of the pipe, aimed at identifying changes in its geometry, was simplified. After the implementation of the aforesaid simplification measures, it was possible to unambiguously evaluate the effects of pressure and temperature on changes in the pipe diameter.

With the gravity of the pipe and of the saddle supports being neglected, at a pressure of 5 MPa and a temperature of 20 °C, the observed diameter strain was $\delta = 0.428$ mm. Resulting values of strain of the metering section of the pipe sized 762 x 25.4 – 1,200 for all the remaining statuses (pressures and temperatures) are listed in Table II.

Another purpose of a stress–strain analysis of the measurement pipe section was to obtain data on stress values along the thickness of the pipe wall. The result of the analysis is presented in Fig. 4. Maximum stress for Calculation Status 2), i.e. at a pressure of 5 MPa and a temperature of 20 °C, while considering the effects of gravity, is indicated by red spots on the pipe. A maximum von Misses stress value was 84.28 MPa. In the flange area, the stress was much lower ($\sigma = 31.70$ MPa).

In identical boundary conditions (a pressure of 5 MPa and a temperature of 20 °C, gravity and saddle support being considered), the pipe strain in the axial direction was also examined. In particular, pipe elongation was monitored in the direction of x-axis of the pipe (Fig. 5). In this case, a maximum stress value amounted to 0.361 MPa, and it was observed at the point where a flange was attached to an adjacent pipe section. This adjacent pipe section was only fictively taken into consideration as an effect of the reinforcement of the flange joint. The reinforcement disabled shifts in the direction of x-axis.

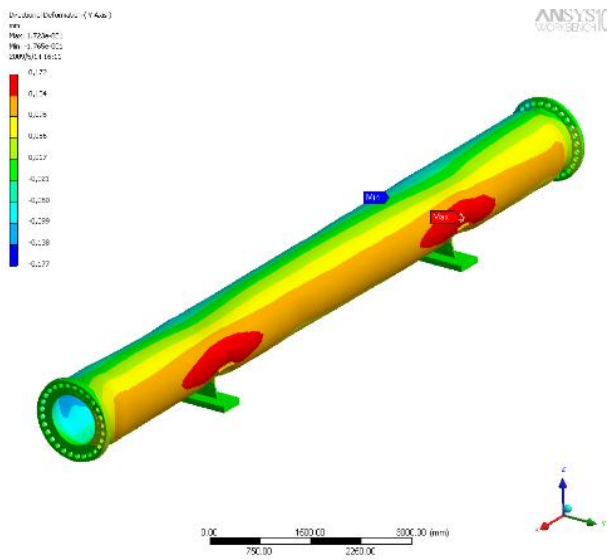

FIGURE 3: Pipe strain without considering gravity (p = 5 MPa; t = 20 °C)

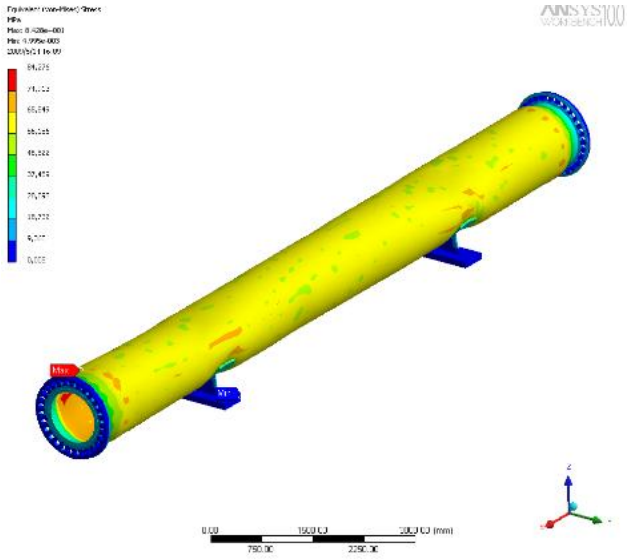

FIGURE 4: Stress-strain status of the pipe with gravity being considered (p = 5 MPa; t = 20 °C)

The strain was also examined in simplified conditions—without considering saddle supports and gravity. In this regard, it was possible to examine only ¼ of the pipe, but for all of the calculation statuses listed above. With the effects of saddle supports, gravity and flanges being excluded from the analysis, the stress identified on the pipe at a pressure of 5 MPa and a temperature of 20 °C is depicted in Fig. 6. A maximum stress value amounted to 86.762 MPa.

The implemented simplification of the boundary conditions had no effects on the accuracy of calculations of changes in the pipe diameter. The application of simplified boundary conditions was based on the principle of elastic deformation of materials, under which even though a pipe shape changes along its circumference, its cross-flow area and hence also a volumetric flow rate of gas do not change.

The investigated factors included the effect of a temperature alone on changes in the pipe diameter; the effect of pressure alone on changes in the pipe diameter; and joint effects of pressure and temperature on changes in the pipe diameter, for all of Calculation Statuses 1) through 4). These effects were examined using ProMechanika, ANSYSE and CosmoseM software environments. The results obtained in all of these environments, in identical boundary conditions, exhibited very good concordance.

Results for the second measurement section of the pipe, which was sized 790 x 19 – 1,200 and examined in identical boundary conditions, are presented in Table III.

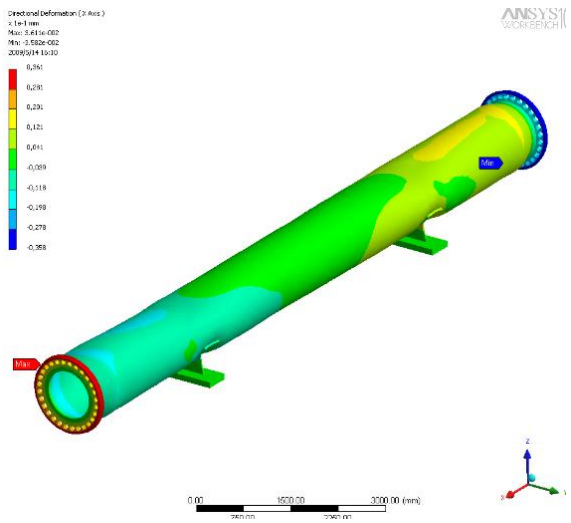

FIGURE 5: Pipe strain in axial direction (p = 5 MPa; t = 20 °C

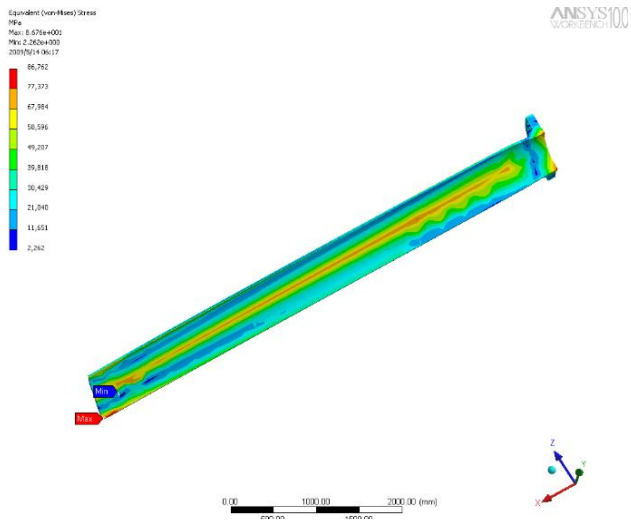

FIGURE 6: Pipe stress without considering gravity and saddle supports (p = 5 MPa; t = 20 °C)

TABLE 2
SUMMARY RESULTS FOR THE PIPE SIZED 762 x 25.4 – 1,200

Summary results of calculations for the measurement section of the pipe						
Nominal dimensions of the pipe	**Nominal inner diameter (mm)**	**Internal pressure (MPa)**	**Gas temperature (^{o}C)**	**Change in diameter (mm)**	**Calculated diameter (mm)**	**Change in pipe length (mm)**
762 x 25.4 – 1,200	711.2	5.0	0	0.251	711.451	-0.814
			15	0.383	711.583	0.186
			20	0.428	711.628	2.519
			25	0.474	711.674	2.799
		5.5	0	0.276	711.476	-1.190
			15	0.407	711.607	0.971
			20	0.453	711.653	1.691
			25	0.498	711.698	2.411
		6.0	0	0.301	711.501	-1.293
			15	0.432	711.632	0.,862
			20	0.477	711.677	1.582
			25	0.523	711.723	2.302
		0.0	0	0.000	711.200	0.000
			15	0.069	711.269	2.160
			20	0.091	711.291	2.880
			25	0.114	711.314	3.600

TABLE 3
SUMMARY RESULTS FOR THE PIPE SIZED 790 x 19 - 1,200

Summary results of calculations for the measurement section of the pipe						
Nominal dimensions of the pipe	**Nominal inner diameter (mm)**	**Internal pressure (MPa)**	**Gas temperature (°C)**	**Change in diameter (mm)**	**Calculated diameter (mm)**	**Change in pipe length (mm)**
790 x 19 – 1,200	752	5.0	0	0.369	752.369	-1.544
			15	0.505	752.505	0.616
			20	0.553	752.553	1.336
			25	0.600	752.600	2.056
		5.5	0	0.406	752.406	-1.699
			15	0.542	752.542	0.462
			20	0.589	752.589	1.182
			25	0.637	752.637	1.902
		6.0	0	0.442	752.442	-1.853
			15	0.578	752.578	0.307
			20	0.626	752.626	1.027
			25	0.667	752.667	1.747
		0.0	0	0.000	752.000	0.000
			15	0.071	752.071	2.160
			20	0.095	752.095	2.880
			25	0.119	752.119	3..600

III. CONCLUSION

The article presents results of investigation into two measurement sections of the natural gas pipeline. The analysis of the effects of pressure alone on pipe deformation revealed an interesting fact. The effect of any pressure at a pipe wall temperature of 0°C always results in a change in the pipe length in the negative direction (pipe length reduction); however, a change in the pipe diameter is positive.

The analysis of the effect of temperature alone on changes in the pipe length indicated that such changes never depend on the pipe diameter; however, they always depend only on a temperature of transported gas (i.e. the temperature inside the pipe). With an increase in the gas temperature, hence also in the temperature of the inner pipe wall, the pipe elongation increases too. The pipe elongation values, measured at identical temperatures, were identical for both pipe diameters.

A particular value of a difference in the pipe diameter, induced by a change in temperature, in the radial direction is directly proportional to the values of a pipe diameter and wall thickness.

ACKNOWLEDGEMENTS

This paper was written with the financial support of the granting agency VEGA within the project solution 1/0626/20 and from FMT VŠB-TUO within the project solutions SP 2022/13.

REFERENCES

[1] V. Ivančo, K. Kubín, K. Kostolný, Program COSMOSM, 2000.

[2] Manual Ansys CFX.

[3] M. Čarnogurská, „Využitie numerických metód pri riešení teplárenského potrubia“. Vytápění, větrání, instalace. Vol. 7, no. 1 (1998), p. 7-9.

[4] M. Čarnogurská, B. Červenka, „Rozloženie tepelných tokov do celozvarovaných výhrevných plôch parných kotlov“. Inženýrská mechanika. Vol. 8, no. 4 (2001), p. 277-285.

AD Publications
Sector-3, MP Nagar, Bikaner,
Rajasthan, India
www.adpublications.org, info@adpublications.org